This is a peer-reviewed, accepted author manuscript of the following article: Inglezakis, V. J., Fyrillas, M. M., & Park, J. (2019). Variable diffusivity homogeneous surface diffusion model and analysis of merits and fallacies of simplified adsorption kinetics equations. *Journal of Hazardous Materials*, *367*, 224-245. https://doi.org/10.1016/j.jhazmat.2018.12.023

Variable diffusivity homogeneous surface diffusion model and analysis of merits and fallacies of simplified adsorption kinetics equations

V.J. Inglezakis[1,2*], M.M. Fyrillas[3], J. Park[4]

[1*]*Nazarbayev University, School of Engineering, Chemical & Materials Engineering Department, Environmental Science & Technology Group (ESTg), Astana, Kazakhstan, e-mail: vasileios.inglezakis@nu.edu.kz*

[2] *The Environment and Resource Efficiency Cluster, Nazarbayev University, Astana, Kazakhstan*

[3]*Frederick University, Department of Mechanical Engineering, Nicosia, Cyprus, e-mail: m.fyrillas@gmail.com*

[4]*University of Wisconsin-Madison, College of Engineering, Civil and Environmental Engineering, USA, e-mail: jkpark@wisc.edu*

Keywords: Adsorption; ion exchange; numerical models; kinetics; batch systems; analytical solutions; HSDM; variable diffusivity

ABSTRACT

Adsorption and ion exchange phenomena are encountered in several separation processes, which in turn, are of vital importance across various industries. Although the literature on adsorption kinetics modeling is rich, the majority of the models employed are empirical, based on chemical reaction kinetics or oversimplified versions of diffusion models. In this paper, the fifteen most

popular simplified adsorption kinetics modelsare presented and discussed. A new versatile variable-diffusivity two-phase homogeneous diffusion model is presented and used to evaluate the analytical adsorption models. Aspects of ion exchange kinetics are also addressed.

1. Introduction

Adsorption and ion exchange processes prevail in separation technologies utilized across different industries, and they are important for wastewater and water treatment. In both processes, porous solids are employed, and thus diffusional mass transfer is the dominant mechanism of sorption. In solids with bi-dispersed pore structures, such as activated carbons and zeolites, macropores act as a path for the adsorbate to reach the interior of the particle. Mass transfer in macropores is typically dominated by molecular and/or Knudsen diffusion and is called pore diffusion. In micropores the adsorbent migrates on the surface of the adsorbent and the mechanism is called surface diffusion [1]. Adsorption of species from a fluid phase into a porous solid is comprised of three steps: (1) mass transfer by diffusion from the bulk fluid phase through the boundary fluid film to the solid's external surface (film diffusion), (2) mass transfer by diffusion into the solid phase (intraparticle diffusion) by in series or in parallel pore diffusion and surface diffusion, and (3) adsorption (physical or chemical) on the solid's surface. Ion exchange follows the same steps and is typically described using adsorption diffusion models. Nevertheless, it is important to underline that adsorption and ion exchange exhibit one major difference, namely the stoichiometric character of the later. Any ions which leave the solid phase are replaced by an equivalent number of ions coming from the liquid phase as a consequence of the electroneutrality requirement [2]. Due to the importance of adsorption and ion exchange in a

variety of processes, kinetics models have been published in numerous papers for over a century. The models can generally be classified as reaction kinetics-based and diffusion-based models.

Any single or combination of steps can be the controlling mechanism, but in porous materials, the adsorption step is typically much faster than the intraparticle diffusion. It is assumed that equilibrium between fluid and solid is instantaneously reached [3]. In ion exchange, the overall rate can be controlled by a chemical reaction but diffusion-controlled processes are more common. In fact, many ion exchange interactions do not involve any direct chemical reaction [2]. This predominance of the solid phase diffusion step in porous solids has not received the desired attention [4]. Diffusion-based models involve partial differential equations and unless the boundary conditions and equilibrium relationship are simple, their solution requires specialised software or the development of numerical methods. It is true that in many occasions, these options are either not readily available or it is impractical to use them, so researchers and industry practitioners prefer simple relations that can be solved quickly and easily. The virtue of simplified models is that the computational complexity is absent and the analytical expression involves only an algebraic equation in closed form which is easily used [5].

There is a variety of analytical and approximate solutions to the diffusion-based models, and empirical equations are extensively used in the literature [1,6,7]. However, in many occasions, these simplified models are used without observing the underlying assumptions, namely the mechanism of diffusion, boundary conditions and equilibrium relationships. Besides the assumptions, different forms of the same solutions to the models and incomplete or wrong definitions of involved variables add to the confusion. The result is the proliferation of mistakes in calculations and the propagation of these mistakes in the literature.

A characteristic example is the Weber-Moris model published in 1963 which has been used numerous times in the literature for liquid phase adsorption [3,8]. The persistence of this model in literature is such that there are papers dedicated to its application on experimental data, as for example the work of Malash and El-Khaiary [9]. Recently, Tran et al. [10] published an excellent work on several repeated mistakes in adsorption literature. However, in the section on adsorption kinetics, several reaction kinetics-based models and only a single diffusion-based model, that of Weber and Moris, are presented. The equation is:

$$\bar{q_t} = k_p \cdot t^{0.5} + \delta \quad (1)$$

where $\bar{q_t}$ is the average loading of the solid phase, k_p is a rate constant of the intraparticle diffusion and δ is a constant associated with the thickness of the fluid's boundary layer. Tran et al. [10] stated that this model can be useful for identifying the reaction pathways and adsorption mechanisms and predicting the rate-controlling step. However, this model is not related to any reaction and it can be easily proved that is only valid at the beginning of the batch adsorption process, under constant bulk fluid concentration (infinite solution volume), absence of liquid phase resistance and linear isotherm; thus, its usefulness, if any, is very limited [3,11].

Reaction kinetics-based models are suitable when a surface reaction takes place, i.e., in chemisorption. Despite the fact that physical adsorption as well as most of the ion exchange processes, are purely mass transfer phenomena [2] reaction kinetics-based models are used extensively in the literature to model and interpret the adsorption kinetics and rate-limiting steps [8,12–14]. These models are typically empirical and most of them ignore the mass transfer mechanisms present in all heterogeneous systems. In an influencial paper published in 1998, Ho and McKay [15] correctly state that diffusion-based models are extremely important particularly in processes where ion exchange and ionic bonding are not as prevalent as in chemisorption

processes. In the same paper, the authors argue that the reaction kinetics-based models can be used to investigate the mechanism of sorption and potential rate controlling steps, such as mass transport and chemical reaction processes. However, as these models ignore diffusion are not able to interpret the sorption mechanisms. Furthermore, being empirical models, even if the fit to the experimental data is acceptable, they are suitable as a descriptive but not as a predictive tool [16]; in other words, the ability of a model to fit experimental data is not sufficient to validate the underlying mechanism [17,18]. The fundamental problem of these models, especially when applied on physisorption and ion exchange, is the absence of any physical significance and the limited usefulness of the empirical kinetic parameters derived by their application on experimental data [19]. Several studies have highlighted the pitfalls of reaction kinetics-based models advocating the use of diffusion-based models [11,14,20–24].

The published review papers on adsorption kinetic models are addressing: (i) only some of the reaction kinetics-based models, basically pseudo-first, pseudo-second order and Elovich equations [15,25] (ii) focus on reaction-kinetics models discussing only a few approximate diffusion-based models [4,13,26,27], or (iii) discuss solely analytical and approximate solutions of diffusion-based models [28,29]. Also, there is a lack of a systematic quantitative study on the comparison of simplified diffusion models with complete numerical models. Such a study requires the use of complex variable diffusivity models equipped with non-linear isotherms. Recently, Marban et al. [24] presented a variable diffusivity diffusion-based model. The authors claimed that no kinetic model for the adsorption onto porous solids that considers the dependence of the diffusion coefficient on the surface coverage has ever been fully solved.

The present paper fills the gap in the literature of adsorption kinetics by presenting, analyzing and comparing both the available diffusion-based and reaction kinetics-based models. The merits

and pitfalls of all models are discussed; as Tran et al. [10] correctly state, the observation and discussion of inconsistencies and mistakes can prevent their propagation in scientific knowledge. Thus, a review on mistakes related to adsorption kinetics and the presentation of the sound approaches is valuable to the scientific community. Also, this study comes to contribute by presenting a new versatile variable diffusivity diffusion-based model, which is used to discuss and evaluate the analytical and approximate models. In comparison to previously published studies, this model can deal with both increasing and decreasing surface diffusion coefficients with increasing solid loading. To the best of our knowledge, this combination is for the first time presented in the literature.

2. Mass transfer diffusion-based models

Diffusion-based models differ in the combinations of the mass transfer resistances, i.e., fluid film, pore fluid (macropore) and surface (micropore) diffusion steps. In addition, they assume an absence of chemical reactions. If a chemical reaction occurs, then reaction-diffusion models, such as the shrinking core model, are consistent with the physical reality and should be considered (see section 3).

The complete diffusion-based model takes into account all diffusion steps in the solid phase and is called heterogeneous pore and surface diffusion model (PSDM). The variants of the complete model are the pore diffusion model (PDM), which assumes that pore diffusion is predominant, and the homogeneous surface diffusion model (HSDM), which assumes that surface diffusion is predominant [14,30,31]. HSDM is more common and models the solid phase as a homogeneous medium. When fluid film is taken into account, these models are called two-phase models (TP) (Figure 1). In the present paper, the HSDM, its TP form and aspects of the PSD are discussed.

When the isotherm is linear, the two models are mathematically equivalent. For a detailed analysis of the PSDM, see elsewhere [14,32].

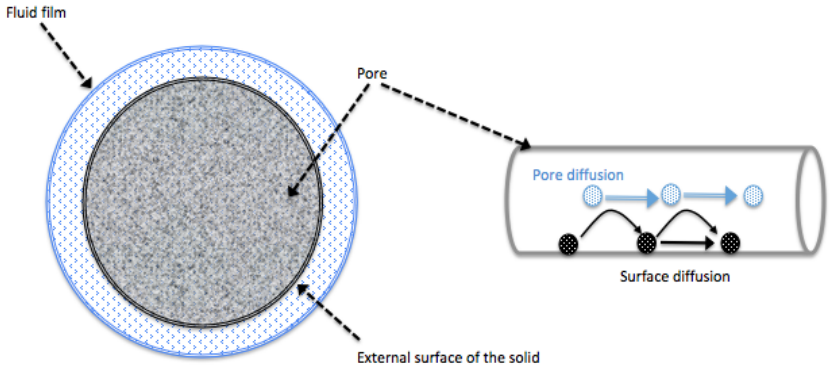

Figure 1. PSDM graphical representation.

The common assumption in adsorption diffusion–based models is that the local adsorption kinetics are much faster than the diffusion process in the solid phase. When the solute reaches the adsorption site, local equilibrium is instantaneously attained even though the fluid phase concentration at the external surface of the solid (HSDM) a within the particle (PSD) change over time. The term "local" identifies that the particular condition is only applicable to a given position, and as time approaches infinity ($t \rightarrow \infty$) and the concentration gradients in the solid disappear, the local equilibrium becomes global equilibrium (isotherm) [33]. The local equilibrium concept is used by the two-film theory of mass transfer for expressing the mass transfer driving forces. Local equilibrium and driving forces are shown in Figure 2 for the HSDM model, where the equilibrium and operating (material balance) lines are plotted. The true bulk phase equilibrium condition is represented by the $\bar{C}_{eq} - \bar{q}_{eq}$ point and depends only on the equilibrium relationship and the material balance. The bars are used to denote average bulk phase concentrations and distinguish them from the local phase concentrations. The bulk phase concentrations of the fluid and solid phases at time (t) are represented by the $\bar{C}_t - \bar{q}_t$ point on the

operating line. The fluid phase concentration at the fluid-solid interface is $C_{t,r=rp}$ and corresponds to the equilibrium solid phase concentration of $q_{t,r=rp}$. According to the two-film theory representation, the driving force in the fluid film is ($\bar{C}_t$-$C_{t,r=rp}$) and is used to express the mass transfer rate in the fluid film in all diffusion-based models. The driving force in the solid film ($q_{t,r=rp}$- $\bar{q}_t$) is called linear driving force approximation (LDF) and it is used in Glueckauf's model which is discussed in section 2.7. Thus, in the general case, on the fluid-solid interface, the fluid and solid phase local equilibrium concentrations are time-dependent (see Figure 9). In this sense, local equilibrium concept is just a convenient way to connect the local fluid and solid phase time-dependent concentrations [21,24] and the description "*equilibrium liquid phase concentration at time t*" can be used for clarity [34].

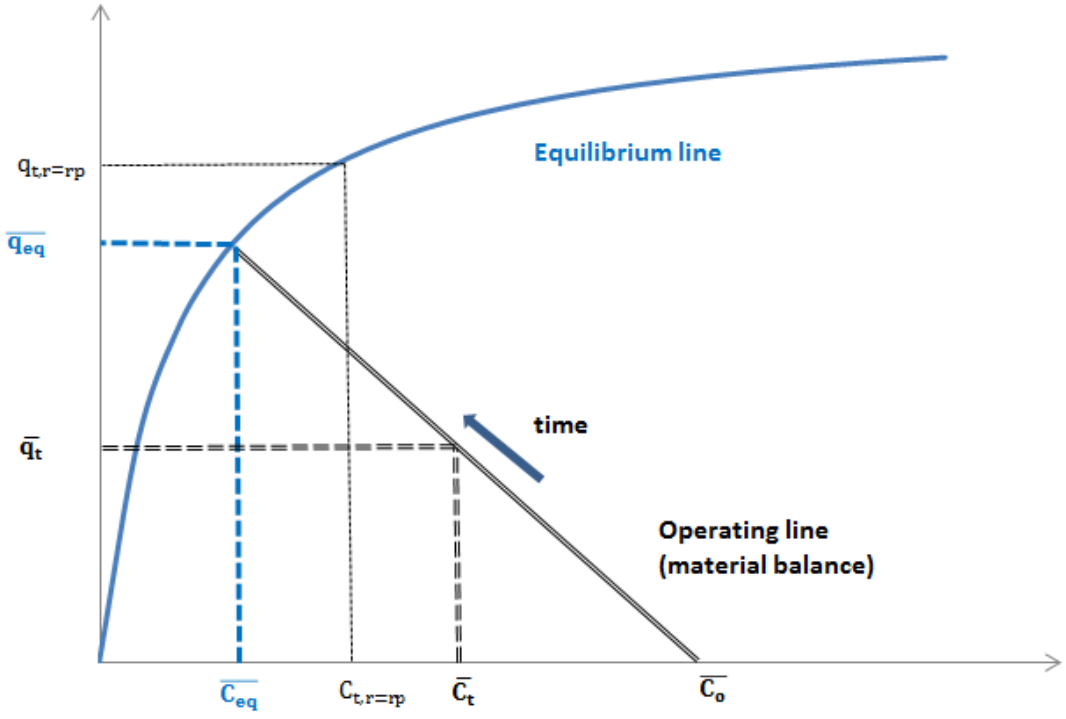

Figure 2. Equilibrium line and the operating line (material balance).

2.1 Two-Phase Homogeneous Surface Diffusion Model

In the TP-HSDM for batch systems, the pertinent assumptions are dilute solutions (trace systems), isothermal process, perfect mixing, spherical particles, single component (adsorption) or binary system (ion exchange), and instantaneous local equilibrium at the fluid-solid interface. The mass balance in a batch reactor is [35]:

$$M \cdot \frac{d\bar{q}_t}{dt} = -V_L \cdot \frac{d\bar{C}_t}{dt} \tag{2}$$

where $\bar{q}_t$ and $\bar{C}_t$ are the average solid and fluid phase concentration at time t, M is the solid mass and V_L is the fluid volume. The initial conditions are: $\bar{C}_{t=o} = \overline{C_o}$ and $\bar{q}_{t=0} = 0$, where $\overline{C_o}$ is the fluid phase initial concentration. The term solid phase concentration is used for the adsorbed (immobilized) solute concentration and should not be confused with the free solute concentration inside the pores of the solid phase.

By integrating equation (2) from t = 0 to t:

$$\bar{q}_t = -\frac{V_L}{M} \cdot (\overline{C_o} - \bar{C}_t) \tag{3}$$

The mass transfer rate in the fluid film is:

$$\frac{\partial \bar{q}_t}{\partial t} = \frac{3 \cdot k_f}{r_p \cdot \rho_p} \cdot \left(\bar{C}_t - C_{t,r=r_p}\right) \tag{4}$$

where k_f is the fluid film mass transfer coefficient, r_p is the particle radius, ρ_p is the particle density and $C_{t,r=rp}$ is the local fluid phase solute concentration at the surface of the solid which is related to the local adsorbed solute concentration at the surface of the solid ($q_{t,r=rp}$) by the equilibrium relationship (Figure 2):

$$q_{t,r=r_p} = f(C_{t,r=r_p}) \tag{5}$$

The solid phase mass transfer rate is an unsteady state diffusion process expressed by the Fick's second law, which in radial coordinates is:

$$\frac{\partial q}{\partial t} = \frac{1}{r^2} \cdot \frac{\partial}{\partial r}\left(D_s \cdot r^2 \cdot \frac{\partial q}{\partial r}\right) = \frac{D_{s,o}}{r^2} \cdot \frac{\partial}{\partial r}\left[D_s(q) \cdot r^2 \cdot \frac{\partial q}{\partial r}\right] \tag{6}$$

where r is the distance from the solid's center. The concentration-dependent surface diffusion coefficient D_s is defined as:

$$D_s = D_{so} \cdot D_s(q) \tag{7}$$

where D_{so} is the constant zero-loading surface diffusion coefficient and $D_s(q)$ is a correlation (see section 2.3). If the surface coefficient is constant then $D_s(q)=1$, $D_s = D_{so}$ and the equation (6) becomes the constant diffusivity model:

$$\frac{\partial q}{\partial t} = \frac{D_s}{r^2} \cdot \frac{\partial}{\partial r}\left(r^2 \cdot \frac{\partial q}{\partial r}\right) \tag{8}$$

where D_s the constant solid phase diffusion coefficient. The average diffusion coefficient is calculated as follows:

$$D_{s,avr} = \frac{D_{so}}{\overline{q_\infty}} \cdot \int_0^{\overline{q_\infty}} D_s(q)dq \tag{9}$$

where $\overline{q_\infty}$ is the equilibrium average solid phase concentration. Note that the solid phase concentrations in equation (6) are local, while in the material balance (equation 3), average concentrations are used. The average solid phase concentration is [36]:

$$\bar{q}_t = \frac{3}{r_p^s} \cdot \int_0^{r_p} q \cdot r^2 dr \tag{10}$$

The solid phase equations (6) and (10) can be combined in order to express the solid phase mass transfer rate in terms of the average solid concentration, which then can be used with the material balance. By differentiating the last equation and using the solid mass transfer rate expression (equation 6):

$$\frac{\partial \bar{q}_t}{\partial t} = \frac{3 \cdot D_{so} \cdot D_s(q_{t,r=r_p})}{r_p} \cdot \left(\frac{\partial q}{\partial r}\right)_{r=r_p} \tag{11}$$

For constant diffusivity:

$$\frac{\partial \bar{q}_t}{\partial t} = \frac{3 \cdot D_s}{r_p} \cdot \left(\frac{\partial q}{\partial r}\right)_{r=r_p} \tag{12}$$

Due to symmetry the boundary condition at the center of the particle (r=0) is:

$$\left(\frac{\partial q}{\partial r}\right)_{r=0} = 0 \tag{13}$$

The boundary condition at the external surface of the particle ($r = r_p$) depends on the mass transfer controlling steps. For combined resistances, i.e., solid and fluid film mass transfer resistances, the rates at $r = r_p$ become equal (no accumulation at the solid surface) and from equations (4) and (11):

$$\frac{3 \cdot D_{so} \cdot D_s (q_{t,r=r_p})}{r_p} \cdot \left(\frac{\partial q}{\partial r}\right)_{r=r_p} = \frac{3 \cdot k_f}{r_p \cdot \rho_p} \cdot \left(\bar{C}_t - C_{t,r=r_p}\right) \tag{14}$$

2.2 Two-Phase Pore Diffusion Model

While in TP-HSDM, there is no fluid in the solid phase and only the adsorbed phase of the solute exist, in TP-PDM the pores are filled with the fluid and the free solute diffuses into the solid phase. As a result, while in TP-HSDM, local equilibrium takes place at the solid's external surface, and in TP-PDM, local equilibrium takes place in all points of the solid phase and the local concentrations at time t are related using the equilibrium equation:

$$q_{t,r} = f(C_{t,p}) \tag{15}$$

where $C_{t,p}$ is the free solute concentration in the pores of the solid, which is in local equilibrium with the adsorbed solute concentration ($q_{t,r}$). TP-PDM also differs in the expression of the solid phase mass transfer equation (Ruthven, 1984):

$$\rho_p \cdot \frac{\partial q}{\partial t} + \varepsilon_p \cdot \frac{\partial C_p}{\partial t} = D_p \cdot \left(\frac{\partial^2 C_p}{\partial r^2} + \frac{2}{r} \cdot \frac{\partial C_p}{\partial t}\right) \tag{16}$$

where D_p is a constant pore diffusion coefficient and (ε_p) is the pore volume of the solid phase. This equation can be written as follows:

$$\left(\rho_p \cdot \frac{\partial q}{\partial C_p} + \varepsilon_p\right) \cdot \frac{\partial C_p}{\partial t} = D_p \cdot \left(\frac{\partial^2 C_p}{\partial r^2} + \frac{2}{r} \cdot \frac{\partial C_p}{\partial t}\right) \tag{17}$$

A variable pore diffusion coefficient is defined as:

$$D_{p,var} = \frac{D_p}{\rho_p \frac{\partial q}{\partial C_p} + \varepsilon_p} \tag{18}$$

Then equation (17) becomes:

$$\frac{\partial C_p}{\partial t} = D_{p,var} \cdot \left(\frac{\partial^2 C_p}{\partial r^2} + \frac{2}{r} \cdot \frac{\partial C_p}{\partial t}\right) \tag{19}$$

where $\frac{\partial q}{\partial C_p}$ is the slope of the equilibrium curve. Note that although the pore diffusion coefficient is constant, the $D_{p,var}$ is variable unless the isotherm is linear. However, this variability has no physical cause as in the case of the surface diffusivity, something that has created confusion in literature. Another equivalent form of equation (16) is:

$$\left(\rho_p + \varepsilon_p \cdot \frac{\partial C_p}{\partial q}\right) \cdot \frac{\partial q}{\partial t} = D_p \cdot \left(\frac{\partial^2 C_p}{\partial r^2} + \frac{2}{r} \cdot \frac{\partial C_p}{\partial t}\right) \tag{20}$$

Under the condition of low pore fluid concentration and very favorable equilibrium the above equation becomes:

$$\rho_p \cdot \frac{\partial q}{\partial t} = D_p \cdot \left(\frac{\partial^2 C_p}{\partial r^2} + \frac{2}{r} \cdot \frac{\partial C_p}{\partial t}\right) \tag{21}$$

The boundary conditions at r = 0 and r = r_p are [35]:

$$\left(\frac{\partial C_p}{\partial r}\right)_{r=0} = 0 \tag{22}$$

$$D_p \cdot \left(\frac{\partial C_p}{\partial r}\right)_{r=r_p} = k_f \cdot \left(\bar{C}_t - C_{t,r=r_p}\right) \quad (23)$$

TP-PDM is more complex than the TP-HSDM as equilibrium is considered in all points in the solid phase. In the case of linear isotherm, the PDM is mathematically equivalent to the HSDM [1,28,36]. Ocampo-Perez et al. [20] compared HSDM and PDM for the adsorption of phenol from aqueous solution onto organobentonite. The authors concluded that although both models fit the experimental data well PDM results in a pore phase diffusion coefficient that is greater than the molecular diffusivity of phenol in water, which is unreasonable. On the contrary, HSDM gives a reasonable surface diffusion coefficient with expected dependence on the experimental conditions. Souza et al. [14] compared the PSDM, HSDM and PDM for the adsorption of a dye on bentonite. PSDM gave the best results, HSDM satisfactory results and PDM failed. In general, PDM is suitable for describing gas phase adsorption in mesoporous-macroporous materials such as silica and alumina while HSDM is more often used for liquid phase adsorption and microporous-mesoporous materials such as zeolites. For further information on the relative importance of surface and pore diffusion, see in Do and Rice [37].

2.3 Variable surface diffusivity correlations

The dependence of surface diffusion coefficient on the solid phase loading is discussed in several publications and, in many systems, is accepted as a fact. This practically means that the surface diffusion coefficient depends on the fluid phase concentration and more general on the conditions outside the solid structure. This is contrary to the classic approach which considers it as a constant for a specific system, i.e., function of temperature, solid's internal structure and incoming species properties.

There are several variable diffusivity correlations and detailed analysis that can be found in Do [33] and Choi et al. [38]. The equation presented by Chen and Yang [39] is the most useful as it has sound theoretical basis and covers both increasing and decreasing trends of the surface diffusion coefficient. The equation is:

$$D_s(\theta) = \frac{1-\theta+\frac{\lambda}{2}\theta(2-\theta)+H[1-\lambda](1-\lambda)\frac{\lambda}{2}\theta^2}{\left(1-\theta+\frac{\lambda}{2}\theta\right)^2} \quad (24)$$

where θ is the dimensionless surface coverage equal to q_t/Q_m, Q_m the saturation capacity of the solid, λ the blockage parameter (whose value indicates the degree of pore blocking by the adsorbate), and H(1- λ) is the Heaviside step function. If $\lambda \geq 1$ then $H[1-\lambda] = 0$ and if $\lambda < 1$ then $H[1-\lambda] = 1$.

The blockage parameter in the Chen-Yang equation indicates the degree of pore blocking of the solid's pores by the adsorbate; λ > 0 indicates hindered diffusion, a situation common in zeolites and λ = 0 means unhindered surface diffusion [39]. Additionally, the surface diffusion coefficient is increasing at λ < 1, has a mixed trend at λ > 1, and practically decreases with solid loading at λ > 5 (Figure 3). For λ = 0the well-known Darken equation for systems following the Langmuir isotherm is derived:

$$D_s(\theta) = \frac{1}{1-\theta} \quad (25)$$

Darken's theory states that the surface diffusion coefficient depends on the equilibrium isotherm between the two phases and it is equal to the value at zero-loading multiplied by a thermodynamic correction factor [33]:

$$D_s(\theta) = \frac{\partial(\ln C_{eq})}{\partial(\ln q_{eq})} \quad (26)$$

This factor is a function of the slope of the isotherm equation and for Langmuir isotherm is equal to $(1-\theta)^{-1}$ and equation (25) is derived. For linear isotherm, the slope is 1 and the surface diffusion coefficient is constant. Note that the Chen-Yung model does not take into account the equilibrium and there is no λ that gives $D_s(\theta) = 1$.

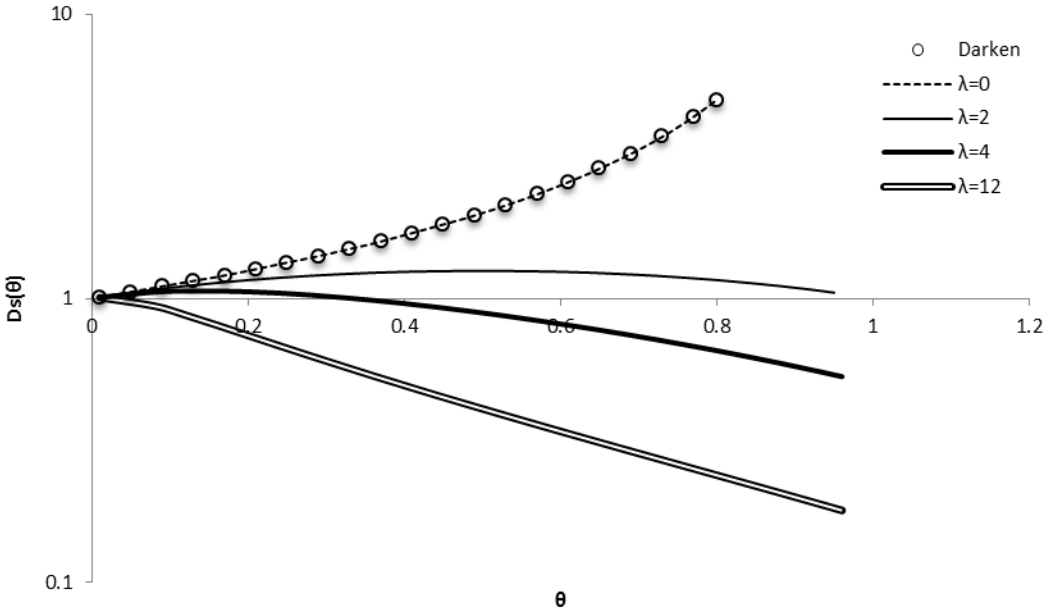

Figure 3. Effect of (λ) on the surface diffusion coefficient.

Ko et al. (2005) [40] studied the batch sorption kinetics of metal ions on bone char and found that surface diffusion coefficients were increasing with solid loading. They applied a constant diffusivity diffusion-based model in combination to Langmuir and Sips isotherms. Several one-parameter variable diffusivity correlations, which is suitable for systems where surface diffusion coefficients increase with surface coverage, were compared. Yang et al. [41] presented a variable diffusivity TP-HSDM model in combination to Fritz–Schlünder isotherm and it was evaluated using experimental data of toluene and dye adsorption on activated carbon. The variable diffusivity correlation used was a simple exponential, suitable for systems where surface diffusion coefficient is increasing with the increase of the solid loading. Marban et al. [24]

studied the removal of a protein onto mesoporous materials and observed the opposite trend, i.e., decrease of surface diffusion coefficient with increasing surface coverage. They applied a variable diffusivity TP-HSDM model in combination to Redlich-Peterson isotherm. The variable diffusivity correlation used in Marban et al. is empirical and involves, apart from (D_{so}) two more adjustable parameters. In the present paper, a variable diffusivity TP-HSDM model in combination to a double-selectivity equilibrium model (DSM) is used. In comparison to previously published studies, this model is equipped with the Chen-Yang variable diffusivity correlation, which can deal with both increasing and decreasing surface diffusion coefficients with increasing solid loading while the DSM can handle S-shaped isotherms.

2.4 Equilibrium isotherms

At this point, it is important to further clarify the differences between the solid phase concentrations used in several equations. For a specific adsorption system, the equilibrium isotherm depends only on temperature. It can be constructed by starting with an initial fluid phase concentration ($\overline{C_o}$) and by varying the fluid volume/solid mass ratio (V_L/M). By doing this, several equilibrium $\overline{q_{eq}}$ - $\overline{C_{eq}}$ pairs are generated (Worch, 2012). The maximum possible liquid phase equilibrium concentration is equal to the initial concentration ($\overline{C_o}$), which corresponds to a maximum solid phase equilibrium concentration ($\overline{q_o}$). The procedure is repeated for higher concentrations until the solid phase loading reaches the saturation capacity (Q_m) (Figure 4). It should be noted that the saturation capacity is not always an asymptotic value as in Figure 4, as this depends on the shape of the isotherm. On the other hand, ion exchange equilibrium depends on temperature and total normality due to the concentration-valence effect [42]. The liquid phase concentration of the incoming ion can vary, but it cannot be higher than the total normality [43].

This means that the maximum solid phase equilibrium concentration $\overline{q_o}$ is also the saturation capacity Q_m for the particular total normality and is called maximum exchange level (MEL). An alternative method for the isotherm construction and q_o (or MEL) measurement is the repeated equilibrations method, where the solid phase is stepwise saturated [6,44]. The equilibrium point, $\overline{C_o}$ - $\overline{q_o}$, can also be obtained by a fixed bed experiment, which is essentially a stepwise saturation procedure. Note that, by operating at a constant inlet fluid phase concentration, a fixed bed experiment provides only a single equilibrium point, i.e., $\overline{C_o}$ - $\overline{q_o}$ (or MEL). Also, the discrepancies between equilibrium data obtained in batch and fixed systems must not be overlooked [45].

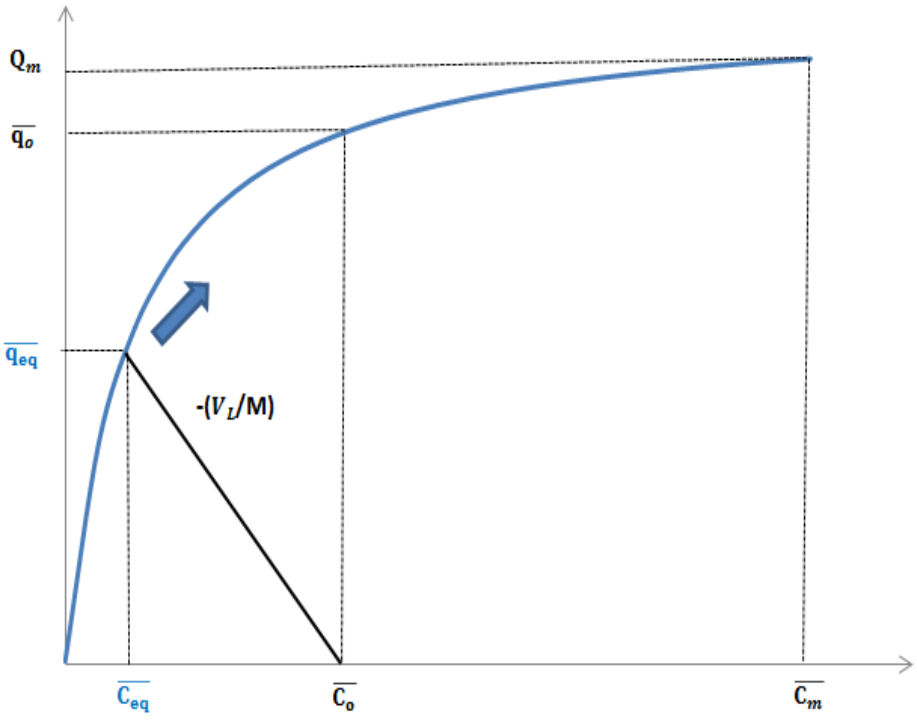

Figure 4. The construction of the equilibrium isotherm. ($-V_L/M$) is the slope of the operating line, expressing the material balance of the system.

Concerning the equilibrium models, of particular interest are the inhomogeneous models which are used to describe multisite (heterogeneous) solid phases behaving differently towards the

same component [45]. A simple approach is to assume that the solid is composed of two distinct regions with no interaction between them. Bricio et al. [46] and later Pepe et al. [47] developed the double-selectivity model (DSM) for heterogeneous ion exchangers using the concept of multisite adsorption. In the case of the exchange of monovalent ions, the derived equation in dimensionless form is [23]:

$$Y_{eq} = p \cdot \frac{K_1 \cdot X_{eq}}{1+(K_1-1)\cdot X_{eq}} + (1-p) \cdot \frac{K_2 \cdot X_{eq}}{1+(K_2-1)\cdot X_{eq}} \quad (27)$$

where $X_{eq} = {C_{eq}}/{\overline{C_o}}$ and $Y_{eq} = {q_{eq}}/{\overline{q_o}}$ are the dimensionless fluid and solid phase equilibrium concentrations, K_1 and K_2 the equilibrium constants, and p the proportion of sites on the solid surface, all positive numbers. Although this equation was derived for the exchange of monovalent ions, it is used in the present paper due to its simplicity and flexibility, as is able to model both Langmurian and S-shaped isotherms. The model can be viewed as two-sites Langmuir isotherm with $La_i = 1/K_i$ [45]:

$$\overline{Y_{eq}} = p \cdot \frac{\overline{X_{eq}}}{La_1+(1-La_1)\cdot \overline{X_{eq}}} + (1-p) \cdot \frac{\overline{X_{eq}}}{La_2+(1-La_2)\cdot \overline{X_{eq}}} \quad (28)$$

2.5 Numerical solution of the variable diffusivity TP-HSDM model

2.5.1 Variable diffusivity TP-HSDM dimensionless numerical model

In a batch reactor kinetics experiment, according to the local equilibrium approach used in kinetics models (Figure 2), the local equilibrium solid phase concentration at the surface $q_{t,r=rp}$ is decreasing from $\overline{q_o}$ to $\overline{q_{eq}}$ and the system eventually reaches the $\overline{q_{eq}}$ - $\overline{C_{eq}}$ point. On the other hand, in fixed bed reactors, the system reaches the $\overline{q_o}$ - $\overline{C_o}$ point. Typically in both operation modes, the part of the isotherms used in the kinetics models is up to the $\overline{q_o}$ - $\overline{C_o}$ point and these

concentrations are typically used for the normalization of the model equations. Nevertheless, any equilibrium point higher than the $\overline{q_o}$ - $\overline{C_o}$ can be used and this can be convenient when kinetics at different initial concentrations are studied. When the whole isotherm is used and the model equations are normalized by using the point $\overline{Q_m}$ - $\overline{C_m}$ the material balance equation and the dimensionless initial condition at t=0 must be adapted accordingly. Note that in this case, $\overline{Q_m}$ and $\overline{C_m}$ replace $\overline{q_o}$ and $\overline{C_o}$ in all equations and dimensionless numbers.

The dimensionless averaged fluid and solid concentrations at any time t are $\overline{X} = {C_t}/{\overline{C_o}}$ and $\overline{Y} = {\overline{q}_t}/{\overline{q_o}}$. The partition ratio Λ is [35]:

$$\Lambda = \frac{M \cdot \overline{q_o}}{V_L \cdot \overline{C_o}} \tag{29}$$

As discussed above, $\overline{q_o} - \overline{C_o}$ is an equilibrium pair and $\overline{q_o}$ is the MEL in ion exchange systems. The dimensionless time (T) is:

$$T = \frac{D_{so} \cdot t}{r_p^2} \tag{30}$$

The Biot number is defined as follows [35]:

$$Bi = \frac{k_f \cdot r_p \cdot \overline{C_o}}{D_{so} \cdot \rho_p \cdot \overline{q_o}} \tag{31}$$

The material balance equation (3) becomes:

$$\overline{Y} = \frac{1}{\Lambda} \cdot (1 - \overline{X}) \tag{32}$$

If the concentration $\overline{C_m}$ is used for the normalization of the model, then the term $(1 - \overline{X})$ must be replaced by the term $(\overline{X}_{T=0} - \overline{X})$.

The fluid phase mass transfer rate equation (4) becomes:

$$\frac{\partial \overline{Y}}{\partial T} = 3 \cdot Bi \cdot (\overline{X} - X_{R=1}) \tag{33}$$

Due to the material balance equation:

$$\frac{\partial \bar{X}}{\partial T} = -3 \cdot \Lambda \cdot Bi \cdot (\bar{X} - X_{R=1}) \tag{34}$$

In the solid phase, mass transfer equation (6) becomes:

$$\frac{\partial Y}{\partial T} = \frac{1}{R^2} \cdot \frac{\partial}{\partial R} \left[R^2 \cdot D_s(Y) \cdot \frac{\partial Y}{\partial R} \right] \tag{35}$$

$R = r/r_p$ is the dimensionless distance from the solid's center. In the expression of D_s the variable Y is used for consistency and thus in equation (24), the surface coverage is $\theta = Y_s \cdot Y$, where $Y_s = {}^{q_o}/_{Q_m}$.

By expanding equation (35):

$$\frac{\partial Y}{\partial T} = D_s(Y) \frac{\partial^2 Y}{\partial R^2} + \frac{\partial D_s(Y)}{\partial R} \frac{\partial Y}{\partial R} + \frac{2}{R} D_s(Y) \frac{\partial Y}{\partial R} \tag{36}$$

where:

$$D_s(Y) = \frac{D_s}{D_{so}} \tag{37}$$

For constant surface diffusion coefficient, $D_s(Y)=1$. The solid phase average concentration equation (10) becomes:

$$\bar{Y} = 3 \cdot \int_0^1 Y \cdot R^2 dR \tag{38}$$

By multiplying both terms of the solid mass transfer rate dimensionless equation (36) by $3 \cdot R^2$ and integrating by use of equation (38), we get:

$$\frac{\partial \bar{Y}}{\partial T} = 3 \cdot D_s(Y_{R=1}) \left(\frac{\partial Y}{\partial R} \right)_{R=1} \tag{39}$$

The initial conditions for T = 0 are $\overline{X}_{T=0} = 1$ and $\overline{Y}_{T=0} = 0$. If another equilibrium point $\overline{q_m}$ - $\overline{C_m}$ is used for the normalization of the model equations then the initial condition at T=0 must be changed to $\overline{X}_{T=0} = \overline{C_o}/\overline{C_m}$. The boundary condition at the center of the solid (R = 0) is:

$$\left(\frac{\partial Y}{\partial R}\right)_{R=0} = 0 \tag{40}$$

At the solid-fluid interface (R=1), local equilibrium is assumed to take place and the dimensionless equilibrium equation is:

$$Y_{R=1} = f(X_{R=1}) \Leftrightarrow X_{R=1} = f^{-1}(Y_{R=1}) \tag{41}$$

For combined solid and fluid phase mass transfer resistances at R = 1, equation (14) becomes:

$$D_s(Y_{R=1}) \cdot \left(\frac{\partial Y}{\partial R}\right)_{R=1} = Bi \cdot (\overline{X} - X_{R=1}) \tag{42}$$

The average surface diffusion coefficient is:

$$D_{s,avr} = \frac{D_{so}}{\theta_\infty} \cdot \int_0^{\theta_\infty} D_s(\theta)d\theta = \frac{D_{so}}{\overline{Y_\infty}} \cdot \int_0^{\overline{Y_\infty}} D_s(Y)d(Y) \tag{43}$$

where $\theta_\infty = Y_s \cdot \overline{Y}_\infty$. The subscript ($\infty$) denotes average bulk phase concentrations at $t \rightarrow \infty$, i.e., after global equilibrium is reached. At global equilibrium, the material balance equation (32) becomes:

$$\frac{1}{\Lambda} \cdot (1 - \overline{X}_\infty) = \overline{Y}_\infty = f(\overline{X}_\infty) \tag{44}$$

$f(\overline{X}_\infty)$ represents the equilibrium relationship, i.e., the DSM model. The above algebraic equation can be solved to obtain an analytical expression for $\overline{X}_\infty$:

$$\overline{X}_\infty = -\frac{a_2}{3\,a_3} - \frac{2^{1/3} \cdot (-a_2^2 + 3a_1 \cdot a_3)}{3a_3(-2a_2^3 + 9a_1 \cdot a_2 \cdot a_3 + 27 \cdot a_3^2 + \sqrt{4(-a_2^2 + 3a_1 \cdot a_3)^3 + (-2a_2^3 + 9a_1 \cdot a_2 \cdot a_3 + 27 \cdot a_3^2)^2})^{1/3}}$$

$$+\frac{(-2\cdot a_2^3+9a_1\cdot a_2\cdot a_3+27\cdot a_3^2+\sqrt{4\cdot(-a_2^2+3a_1\cdot a_3)^3+(-2a_2^3+9a_1\cdot a_2\cdot a_3+27\cdot a_3^2)^2})^{1/3}}{3\,2^{1/3}\cdot a_3} \tag{45}$$

where:

$$a_1 = (3 - K_1 - K_2 + K_2\cdot\Lambda + K_1\cdot\Lambda\cdot p - K_2\cdot\Lambda\cdot p) \tag{46}$$

$$a_2 = (-3 + 2\cdot K_1 + 2\cdot K_2 - K_1\cdot K_2 - K_2\cdot\Lambda + K_1\cdot K_2\cdot\Lambda - K_1\cdot\Lambda\cdot p + K_2\cdot\Lambda\cdot p) \tag{47}$$

$$a_3 = (1 - K_1 - K_2 + K_1\cdot K_2) \tag{48}$$

For a solid phase free of solute at t = 0, the fractional attainment of equilibrium is [6]:

$$U(t) = \frac{\bar{q}_t}{\bar{q}_\infty} = \frac{\bar{Y}}{\bar{Y}_\infty} = \frac{\bar{C}_0 - \bar{C}_t}{\bar{C}_0 - \bar{C}_\infty} = \frac{1-\left(\bar{X}/\bar{X}_{T=0}\right)}{1-\left(\bar{X}_\infty/\bar{X}_{T=0}\right)} \tag{49}$$

If the initial fluid concentration in the kinetics experiment $\bar{C}_o$ is used for the normalization of the concentration, then $\bar{X}_{T=0} = 1$.

2.5.2 Numerical methods

The partial differential equation (36) is spatially discretized using central differences, hence the spatial derivatives are approximated as follows:

$$\frac{\partial Y}{\partial R}[T, R_k] = \frac{Y[T,R_{k+1}] - Y[T,R_{k-1}]}{2\,\delta R} \tag{50}$$

$$\frac{\partial^2 Y}{\partial R^2}[T, R_k] = \frac{Y[T,R_{k+1}] - 2Y[T,R_k] + Y[T,R_{k-1}]}{\delta R^2} \tag{51}$$

$$\frac{\partial D_s(Y)}{\partial R} = \frac{\partial D_s(Y)}{\partial Y}\cdot\frac{\partial Y}{\partial R} \tag{52}$$

where the last equation was obtained using the chain rule, and $\frac{\partial D_s(Y)}{\partial Y}$ can be obtained analytically. The notation used, is common in numerical analyses, and the details can be found in any textbook [48]. Using above notation, equation (36) can be expressed as follows:

$$\frac{dY_k}{dT} = D_s(Y_k) \cdot \frac{Y_{k+1}[T] - 2\,Y_k[T] + Y_{k-1}[T]}{\delta\, R^2} + \frac{\partial D_s(Y)}{\partial Y} \cdot \left(\frac{Y_{k+1}[T] - Y_{k-1}[T]}{2\,\delta\, R}\right)^2 + \frac{2}{R_k} \cdot D_s(Y_k) \cdot \frac{Y_{k+1}[T] - Y_{k-1}[T]}{2\,\delta\, R}$$

(53)

while the material balance equation (34) takes the form:

$$\frac{d\bar{X}_k}{dT} = -3 \cdot \Lambda \cdot \mathrm{Bi} \cdot \left(\bar{X}_k[T] - f^{-1}[Y[T, R = 1]]\right) \tag{54}$$

The system of ordinary differential equations (53) and (54) is solved numerically using the modified Euler method [48]. Two points that need clarification are the way the boundary conditions of equation (36), i.e., equations (40) and (42), are incorporated in the numerical method. Equation (40), the symmetry boundary condition, leads to a division by zero when applied to equation (36) at $R = 0$. This is addressed by applying L' Hôpital's rule to the singular term $\frac{2}{R} \cdot \frac{\partial Y}{\partial R}$, which simplifies to $2\frac{\partial^2 Y}{\partial R^2}$. The non-linear boundary condition equation (42) is made explicit by evaluating the right-hand side on the previous time step, i.e., if i symbolizes the current time step, then,

$$\frac{Y[T_i, R_{k+1}] - Y[T_i, R_{k-1}]}{2\,\delta R} = \mathrm{Bi} \cdot \left(\bar{X}[T_{i-1}] - f^{-1}[Y[T_{i-1}, R_k]]\right) \tag{55}$$

To estimate the distance (error) between two curves, i.e., numerical $\bar{X}(T)$ vs analytical or numerical $\bar{X}(T)$, the standard method is to use the sum of the square of the difference between the dependent variables $\bar{X}(T)$ for the same value of the independent variable (T), i.e., measure the error (distance) parallel to the y-axis. Minimizing this sum is called curve-fitting using the least square approach [48]. This method, also called ordinary least square (OLS), amplifies the error when the curves have large slope even if the distance between them is small. An example is the $U(T)$-T curves for small values of T where they become almost vertical (Figure 5). To alleviate this, the total least squares (TLS), and its special case called Deming regression [49],

can be used where the distance of two curves is measured with respect to the perpendicular distance between them. This accounts for errors on both the x- and y-axes. For simplicity in the present paper an analogous method is used where the error is calculated as the normalized area between the two curves.The normalization parameter is the area above the curve of the numerical solution. In this way, the error does not depend on the curves orientation.

2.5.3. Numerical model results and discussion

Characteristic solutions of the variable diffusivity model for Y_s=1 are shown in Figures 5 (effect of λ) and 6 (effect of D_{so}). As is evident, the effect of (λ) is insignificant at the beginning of adsorption and becomes gradually potent at higher values of (T). This insensitivity of the model at low (T) is due to the relatively fast adsorption at the beginning of the adsorption, mostly controlled by the fluid phase mass transfer resistance. The effect of (D_{so}) is profound, especially when surface diffusion coefficient is below 10^{-8} cm^2/s. Also, in order to compare the solutions in Figures 6 to 8, U(T) is plotted versus to t/r_p^2 (s/cm^2), equivalent to $T/D_{s,avr}$ for the constant diffusivity model and T/D_{so} for the variable diffusivity model.

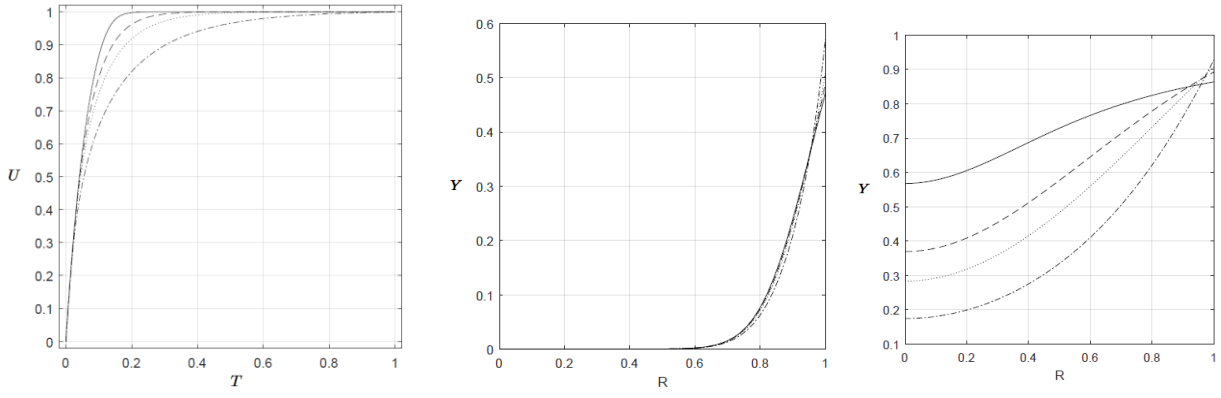

Figure 5. Effect of (λ) on the numerical solution for a DSM favorable isotherm (r = 0.5, K_1 = 12, K_2 = 10), Λ = 0.5 and Bi = 5: λ = 0 (solid curve), λ = 1 (dashed curve), λ = 2 (dotted curve), λ = 5 (dashed-dot curve). Left: U(T)-T, middle Y(R)-R for T = 0.01 and right Y(R)-R for T = 0.1.

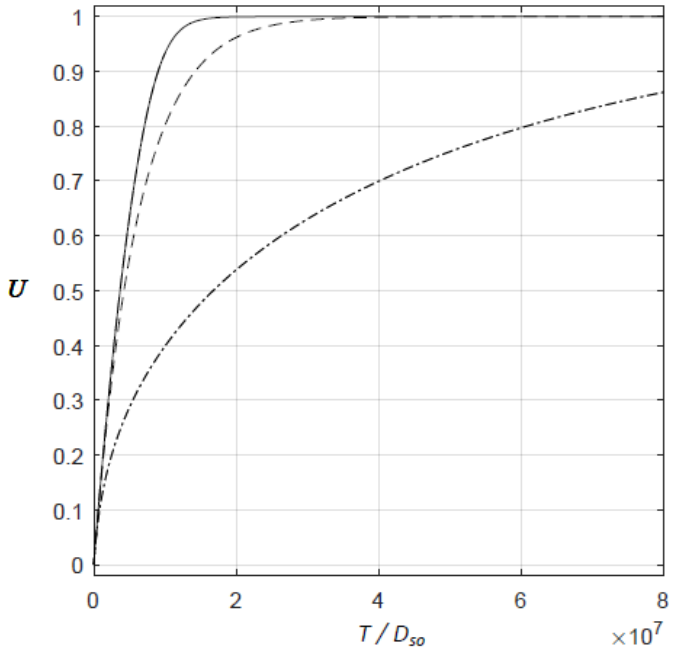

Figure 6. Effect of (D_{so}) on the numerical solution for a DSM favorable isotherm (r = 0.5, K_1 = 12, K_2 = 10), Λ = 0.5 and λ = 1: $D_{so} = 10^{-7}$ (Bi = 0.5, solid curve), $D_{so} = 10^{-8}$ (Bi = 5, dashed curve) and $D_{so} = 10^{-9}$ (Bi=50, dashed-dot curve).

The comparison between variable and constant diffusivity models is made for the favorable isotherm systems shown in Table 1 for Y_s=1. In the constant diffusivity model, the average surface diffusion coefficient of the variable diffusivity model obtained by equation (43) is used.

Table 1. Variable diffusivity systems for a DSM favorable isotherm (r = 0.6326, K_1 = 12.045, K_2 = 5).

	A1	**A2**	**B1**	**B2**	**C1**	**C2**	**D1**	**D2**
Λ (-)	0.01	0.01	0.01	0.01	1	1	1	1
Bi (-)	0.5	0.5	5	5	0.5	0.5	5	5

D_{so} (cm^2/s)	10^{-7}	10^{-7}	10^{-8}	10^{-8}	10^{-7}	10^{-7}	10^{-8}	10^{-8}
λ (-)	0.1	10	0.1	10	0.1	10	0.1	10
$D_{s,avr}$ (cm^2/s)	3.92×10^{-7}	5.32×10^{-8}	3.92×10^{-7}	5.32×10^{-8}	1.81×10^{-7}	6.28×10^{-8}	1.81×10^{-7}	6.28×10^{-8}
Error	0.0036	0.0234	0.0222	0.032	0.0036	0.0223	0.05	0.1974

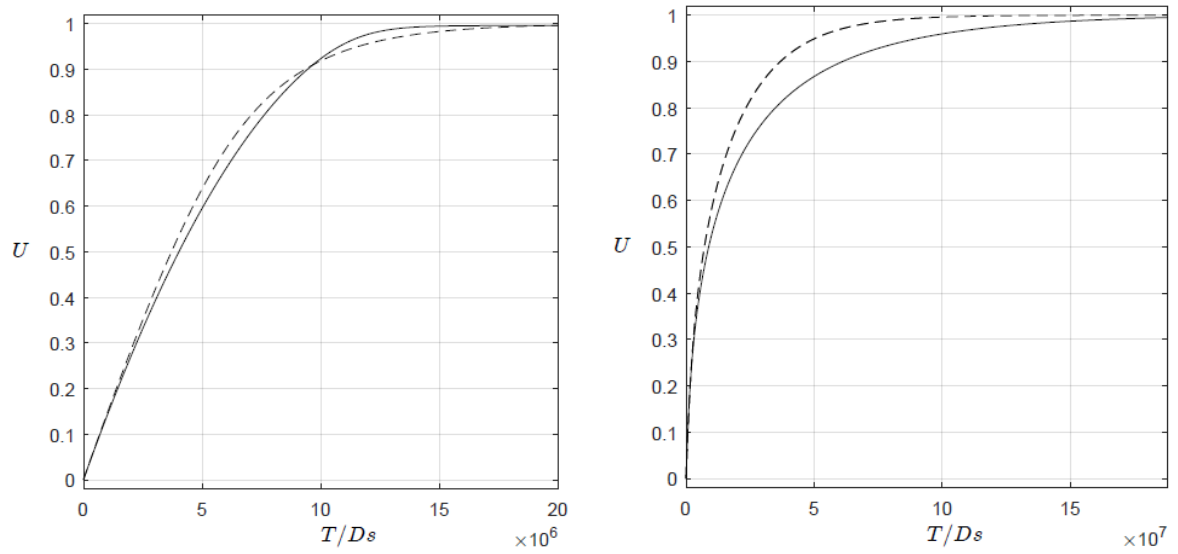

Figure 7. Comparison of constant diffusivity (dotted lines) and variable diffusivity (solid lines) solutions for the infinite solution volume condition and intermediate Biot number for surface diffusion (left, B1) and hindered diffusion (right, B2).

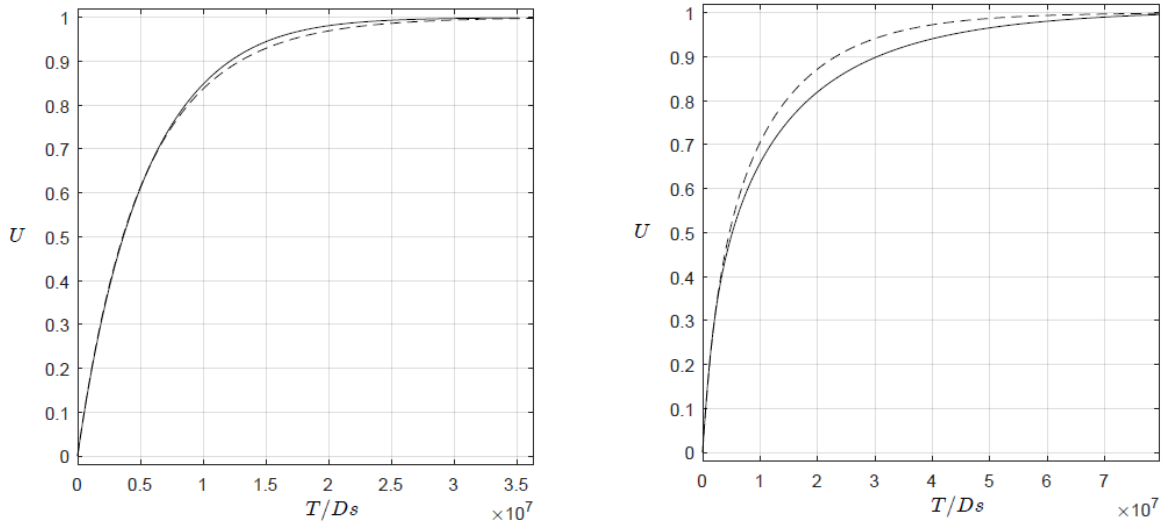

Figure 8. Comparison of constant diffusivity (dotted lines) and variable diffusivity (solid lines) solutions for the finite solution volume condition and intermediate Biot number for surface diffusion (left, D1) and hindered diffusion (right, D2).

The results show that the constant diffusivity solution can be reasonably close to the variable diffusivity solution for U(T) lower than about 0.7. The differences are smaller at low Biot number while the effect of λ depends on the Biot number. Similar results can be obtained for different combinations of parameters. These results show that constant diffusivity model can be used even if the solid phase diffusion coefficient is variable, at least for the first part of the adsorption kinetic curve. Further discussion on this matter is conducted in section 2.7.

2.6 Analytical solutions and comparison to the constant diffusivity HSDM numerical solutions

The solid phase concentration at R = 1 ($Y_{R=1}$) is variable in time leading to time-dependent boundary condition which, in the general case, is non-linear due to the isotherm shape (equation 41). This is shown in Figure 9 where the constant diffusivity HSDM numerical solution Y(R)-R profiles are plotted for surface diffusion control, linear and a favorable equilibrium and three times T = 0.01 (beginning), T = 0.1 (intermediate) and T = 0.3 (near to equilibrium).

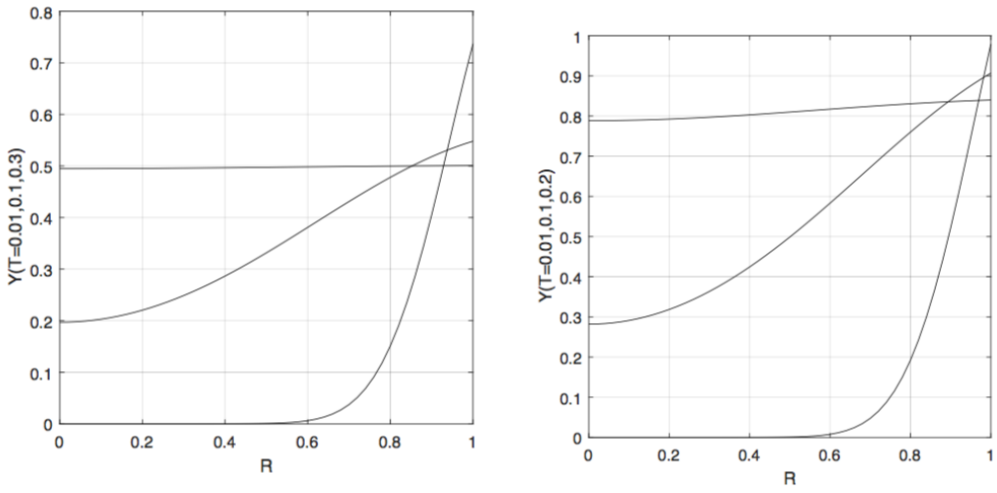

Figure 9. Solid phase concentration profiles for Bi = 100 and Λ = 1 for DSM isotherms. Left: p = 1, K_1 = 1, K_2 = 1 (linear) and right p = 1, K_1 = 25, K_2 = 1 (favorable).

The effect of the isotherm type on the constant diffusivity HSDM solutions is shown in Figure 10. An interesting feature of the U(T)-T curve is that depending on (Λ), the solution of the unfavorable or linear isotherm may approach the equilibrium faster or slower than the favorable isotherm (Figures 10, 20 and 21). This seems controversial, but it should be noted that U(T) expresses the relative rate, while the absolute rate is:

$$-r_k = -\frac{d\overline{C_t}}{dt} = -\overline{C_o}\cdot\frac{d\bar{X}(t)}{dt} = (\overline{C_o} - \overline{C_\infty})\cdot\frac{dU(t)}{dt} \tag{56}$$

or

$$\frac{dU(t)}{dt} = -\frac{\overline{C_o}}{(\overline{C_o}-\overline{C_\infty})}\cdot\frac{d\bar{X}(t)}{dt} \tag{57}$$

Thus, the relative rate of adsorption depends on both the absolute rate and the equilibrium concentration. The absolute rate is represented by the slope of the $\bar{X}(T)$-T curve and the rate of the unfavorable isotherm, as expected, is always lower than the rate of the favorable isotherm (Figure 10).

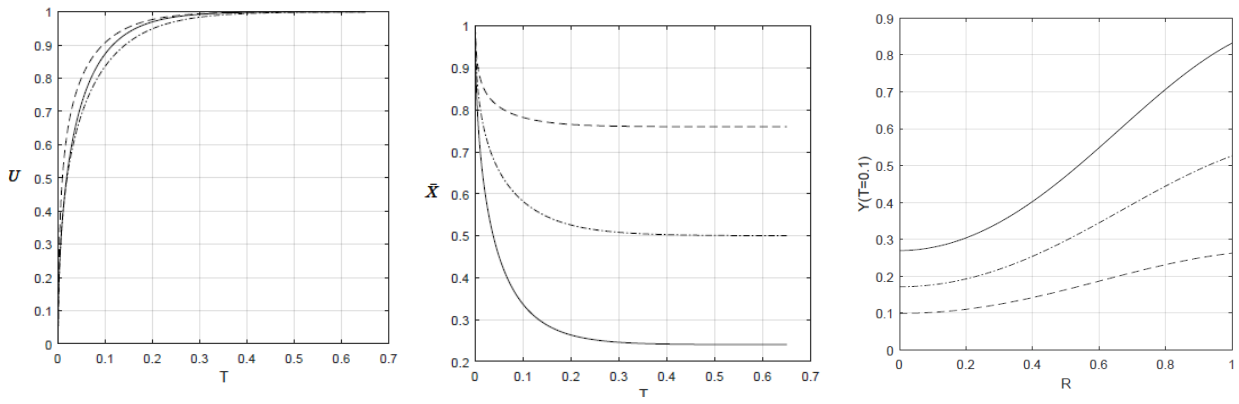

Figure 10. Effect of different isotherms on the numerical solution for Bi = 100, Λ = 1 and DSM favorable isotherm (p = 1, K_1 = 10, K_2 = 1, solid), sigmoidal (r = 0.5, K_1 = 10, K_2 = 0.1, dashed-dot) and unfavorable isotherm (p = 1, K_1 = 0.1, K_2 = 1, dashed).

Due to the boundary condition at the fluid-solid interface, analytical solutions to TP-HSDM and TP-PDM are possible only for constant intraparticle diffusion coefficient and linear or rectangular isotherms. Here, the most common solutions are presented which are those of HSDM and several of PDM, i.e., single controlling mechanism (Table 2). Analytical solutions to the PDM, combined fluid film-solid phase resistances and rectangular isotherms can be found in Weber [28] and Suzuki [1]. The following analysis is done for the TP-HSDM model, unless otherwise specified. The numerical model was validated by comparing its predictions to the HSDM analytical solutions under the conditions shown in Table 2 and constant diffusivity, i.e., $D_s(Y) = 1$.

Table 2. Summary of analytical models

Model (equation)	Boundary condition	Controlling diffusion step	Isotherm type
Boyd (69)	Infinite solution volume $\Lambda < 0.1$	Surface diffusion Bi > 100	Not needed
Boyd (69)	Finite solution volume $\Lambda \leq 1$	Surface diffusion Bi > 100	Rectangular
Crank (60)	Finite solution volume	Surface diffusion Bi > 100	Linear
Perry & Green (76)	Infinite solution volume $\Lambda < 0.1$	Fluid film diffusion Bi < 1	Langmuir
Helfferich (67)	Finite solution volume	Fluid film diffusion Bi < 1	Linear

2.6.1. Linear isotherm

In the case of linear isotherm ($\overline{Y}_{eq} = \overline{X}_{eq}$), the following relationship holds:

$$\frac{\overline{q_\infty}}{\overline{c_\infty}} = \frac{\overline{q_o}}{\overline{c_o}} \tag{58}$$

Then, (Λ) becomes:

$$\Lambda = \frac{1-\overline{X_\infty}}{\overline{X_\infty}} \tag{59}$$

In this case, the boundary condition at R=1 becomes linear, simplifying the solution of the differential equations. The solution's versions found in the literature are derived from this given by Crank [50]:

$$U(T) = 1 - \sum_{n=1}^{\infty} \frac{6 \cdot A \cdot (A+1) \cdot \exp\left(-u_n^2 \cdot T\right)}{9 + 9 \cdot A + (A \cdot u_n)^2} \tag{60}$$

where A = 1/Λ and (u_n) are the roots of the equation:

$$\tan(u_n) = \frac{3 \cdot u_n}{3 + A \cdot u_n^2} \tag{61}$$

Helfferich [6] gives the same equation for isotopic exchange, i.e., ion exchange between isotopes, which is equivalent to linear equilibrium of an adsorption system. Equation (60) holds for PDM as well but (T) should be multiplied by $\overline{C_o}/\rho_p \cdot \overline{q_o}$ [1,35]. In some papers, Crank's equation is named linear adsorption model (LAM) [51–53]. By using the material balance (equation 32), the concentration in the fluid phase can be calculated [35]:

$$\overline{X}(T) = 1 - \frac{1}{1+A} \cdot \left[1 - \sum_{n=1}^{\infty} \frac{6 \cdot A \cdot (A+1) \cdot \exp\left(-u_n^2 \cdot T\right)}{9 + 9 \cdot A + (A \cdot u_n)^2}\right] \tag{62}$$

Ruthven [36]and Perry and Green [54] give the following form of the solution:

$$U(T) = 1 - 6 \cdot \sum_{n=1}^{\infty} \frac{\exp\left(-p_n^2 \cdot T\right)}{\frac{9 \cdot \Lambda_\infty}{1-\Lambda_\infty} + (1-\Lambda_\infty) \cdot p_n^2} \tag{63}$$

where p_n are the roots of the equation:

$$\frac{\tan(p_n)}{p_n} = \frac{3}{3 + \left(\frac{1}{\Lambda_\infty} - 1\right) \cdot p_n^2} \tag{64}$$

Ruthven [36] defines (Λ_∞) as follows:

$$\Lambda_\infty = \frac{M \cdot \overline{q_\infty}}{V_L \cdot \overline{C_0}} = \frac{\overline{C_0} - \overline{C_\infty}}{\overline{C_0}} = 1 - \overline{X_\infty} \tag{65}$$

It should be noted that Ruthven's equation cannot be used when $\Lambda_\infty \to 0$ or $\overline{X_\infty} \to 1$. Both Ruthven and Perry and Green give equation (63) for surface diffusion control and then use the same equation for pore diffusion control and linear isotherm, which is misleading. Also, both

sources do not mention the condition of linear isotherm and, because equations (60) and (63) look different it might be wrongly assumed that the latter is applicable for any isotherm. However, a closer inspection of the equations shows that they are the same if:

$$A = \frac{1}{\Lambda_\infty} - 1 \tag{66}$$

which is true only for a linear isotherm (equation 59). In Figure 11, the equations of Crank (equation 60) and Ruthven (equation 63) are compared to the complete numerical solution. For a linear isotherm, as expected, all models coincide but for non-linear isotherm they all diverge. Note that for non-linear isotherm the $\overline{X_\infty}$ needed for the calculation of Λ_∞ in Ruthven's solution is calculated by using equation (45).

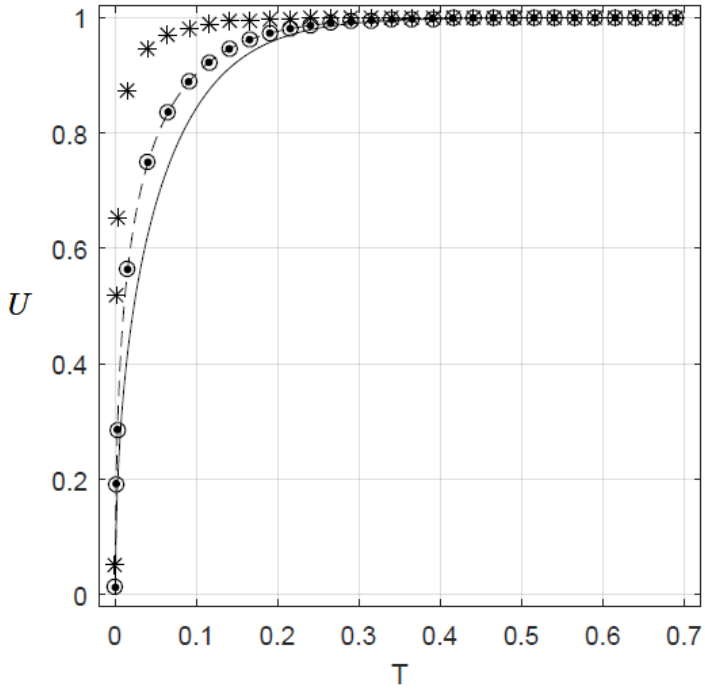

Figure 11. Comparison of the numerical solution (lines), Cranks's equation (dots) and Ruthven's equation (circles for linear and star for non-linear isotherm) for Bi = 1,000 and Λ = 1 for non-linear isotherm (solid curve, DSM: p = 0.5/K_1 = 50/K_2 = 50) and linear isotherm (dashed curve).

The effect of Biot number on the numerical solution is shown in Figure 12. As is clear Crank's model coincides with the numerical model only for linear isotherm and high Biot number, i.e. surface diffusion control condition. Besides this observation, the effect of Biot number is profound for both types of isotherm.

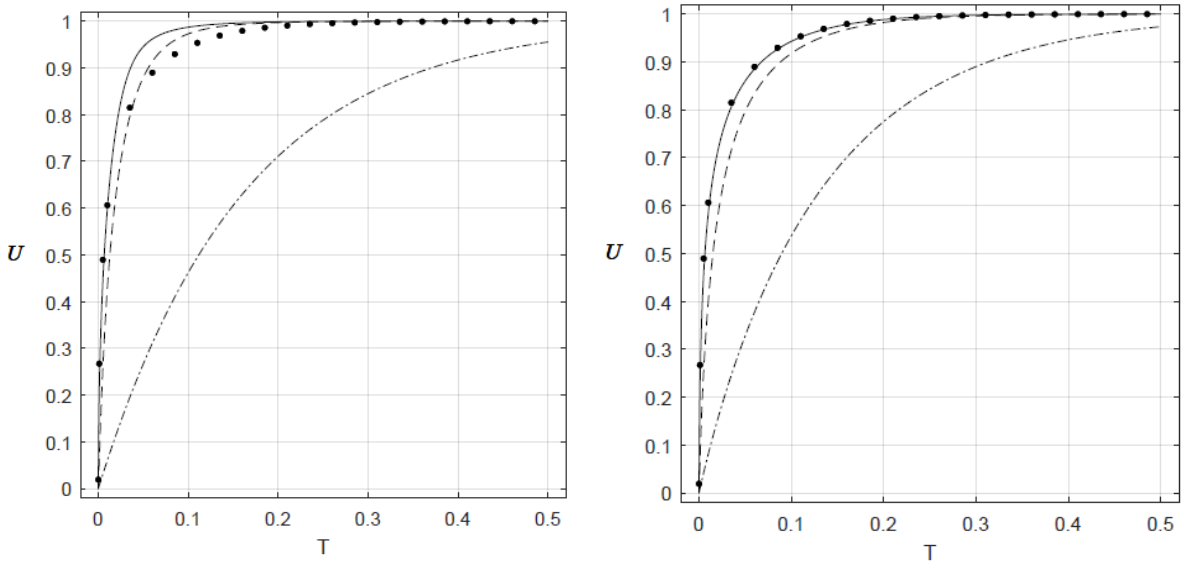

Figure 12. Effect of Biot number on the numerical solution (curves) and on Crank's solution (points) for $\Lambda = 2$ and Bi = 1 (dashed-dot line – fluid film diffusion control), Bi = 10 (dashed line) and Bi = 100 (solid line – surface diffusion control). Left: DSM isotherm ($p = 0.6326/K_1 = 12.045/K_2 = 121.33$) and Right: Linear isotherm.

The preceding equations can be used for any finite value of (Λ), a condition called finite solution volume. Chen et al. [51] and Pritzker [53] successfully applied Crank's equation for the removal of Cu^{2+} on calcium alginate gel. The models presented, as Inglezakis and Grigoropoulou [29] and more recently Schwaab et al. [3] have shown, are not used as often as other simpler ones. Also, the condition of linear isotherm is not always respected, as for example in Kurtoglu and Atun [55], who used Worch's version (equation 62) for the Pb/Na exchange on clinoptilolite that follows non-linear isotherm, Araujo and Teixeira [52] who applied Crank's equation for the

removal of Cr^{3+} on alginate that follows a S-shaped isotherm, Inglezakis and Grigoropoulou [29] who applied a similar to Ruthven's version for the sorption of Pb^{2+} on natural and modified clinoptilolite and Dyer and White [56], who used another version of the same model, called Carman-Haul equation for cations exchange on clinoptilolite without presenting the isotherm. This is discussed further in section 2.7.

Fluid film diffusion control is rarely considered, as adsorption in porous materials is more often controlled by the diffusion in the solid phase. Helfferich [6] gives the following solution for finite solution volume and linear isotherm:

$$U(T) = 1 - \exp[(\Lambda + 1) \cdot (3 \cdot Bi \cdot T)] \tag{67}$$

By using the material balance (equation 32), the concentration in the fluid phase can be calculated [35]:

$$\overline{X}(T) = \frac{1}{\Lambda+1} + \frac{\Lambda}{\Lambda+1} \cdot e^{[-(\Lambda+1)\cdot(3\cdot Bi\cdot T)]} \tag{68}$$

The comparison of numerical and analytical solutions for fluid film diffusion control are provided in Figure 13. The agreement between the models is perfect.

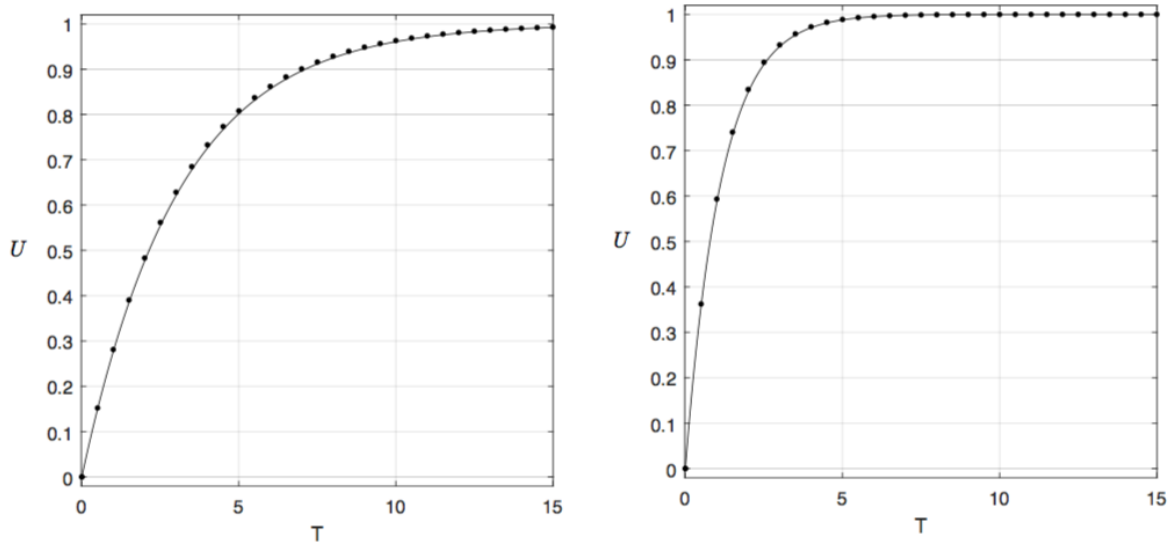

Figure 13. Comparison of the numerical solution (solid line) and Helfferich's equation (points) for Bi = 0.1 and linear isotherm. Left: $\Lambda = 0.1$ and Right: $\Lambda = 2$.

2.6.2 Constant adsorbed phase concentration at the surface of the solid

If the boundary condition at R = 1 is independent of time, solutions of the model are further simplified. This condition is valid in two cases: (a) infinite solution volume and (b) irreversible equilibrium under excess adsorbate in the fluid phase ($\Lambda \leq 1$).

The infinite solution volume condition is reached when $\Lambda \rightarrow 0$ and, in the absence of fluid film resistance, the fluid phase concentration at the external surface of the solid remains constant and equal to the bulk fluid phase concentration ($\overline{C_o}$) at all times [28]. Also, when $(V_L/M) \rightarrow \infty$ the global equilibrium concentrations become equal to the maximum values, i.e., (C_o) and (q_o) (Figure 4). Thus, in the absence of fluid film resistance, the local equilibrium condition at the external surface of the solid is $Y_{R=1} = X_{R=1} = 1$ and at $t \rightarrow \infty$ is $\overline{Y_\infty} = \overline{X_\infty} = 1$. While in pore diffusion control the model solutions still depend on the isotherm curvature, whereas in surface diffusion control the isotherm becomes irrelevant resulting in a single analytical solution (Figure 14) [28]. Because $\overline{Y_\infty} = 1$ from equation (49), $U(T) = \overline{Y}$ while the material balance becomes irrelevant because $\overline{X} = 1$ at all times. Under the infinite solution volume condition, the solution to the HSDM model was given by Boyd [28,54,57]:

$$U(T) = 1 - \frac{6}{\pi^2} \cdot \sum_{n=1}^{\infty} \frac{1}{n^2} \cdot \exp(-n^2 \cdot \pi^2 \cdot T) \qquad (69)$$

The same solution is derived for PDM and linear isotherm but (T) should be multiplied by $\overline{C_o}/\rho_p \cdot \overline{q_o}$ [1].

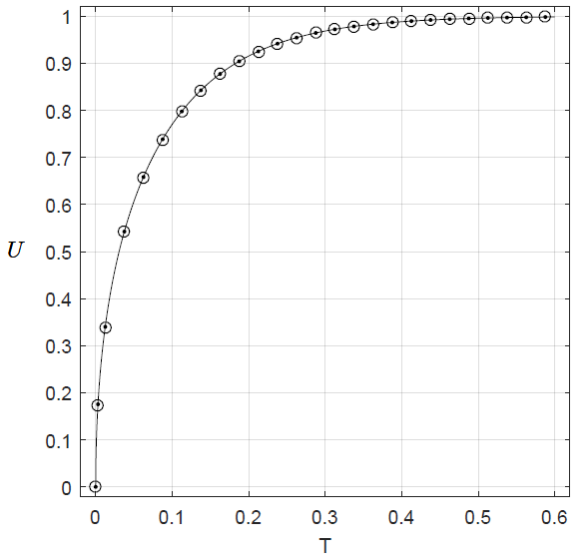

Figure 14. Numerical solution for Bi = 1,000 and $\Lambda = 0.001$ for different DSM isotherms: $p = 0.6326/K_1 = 12.045/K_2 = 121.33$ (strongly favorable – line), $p = 0.6326/K_1 = 12.045/K_2 = 1$ (favorable - points) and $p = 1/K_1 = 1/K_2 = 1$ (linear isotherm - cycles).

The comparison of the numerical solution with Boyd's and Crank's equation for Bi = 1,000 and linear isotherm is shown in Figure 15. All solutions coincide for low (Λ), which is the infinite solution volume condition, while for higher Λ, Boyd's model diverges, and Crank's model coincides with the numerical solution.

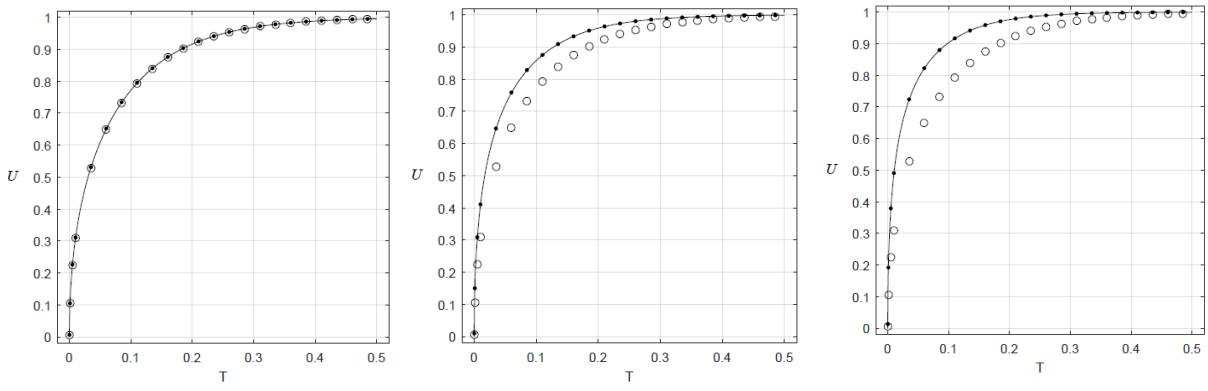

Figure 15. Comparison of the numerical solution (curves), Boyd's equation (circles) and Crank's equation (points) for Bi = 1,000 and linear isotherm: $\Lambda = 0.01$ (left - infinite solution volume), $\Lambda = 0.5$ (middle) and $\Lambda = 1$ (right).

Boyd's equation has been extensively used in adsorption and ion exchange systems, regardless of its obvious limitation of being based on the infinite solution volume condition. This condition implies constant fluid phase concentration and is often overlooked in literature. For instance, it has been applied for the sorption of Cu^{2+} on hydroxyapatite and zeolite [58], several heavy metals on zeolite [59], and freon on activated carbon [60] under finite solution volume conditions.

The rectangular isotherm (irreversible equilibrium) is shown in Figure 16. The equilibrium concentrations depend on Λ. For $\Lambda \leq 1$, the solute amount in fluid phase is equal to or in excess of the amount that the solid phase can take. The equilibrium relationship becomes then $\overline{Y_{eq}} = 1$ regardless the value of $\overline{(X_{eq})}$. Thus, as in the case of infinite solution volume, the amount adsorbed at the external surface of the particle is constant regardless of the decrease of the fluid phase concentration, i.e., $Y_{R=1} = 1$ (Figure 17). Also, the boundary condition at R = 1 is identical to the infinite solution volume condition resulting in identical solutions to the HSDM model [1]. Note that at global equilibrium $\overline{Y_{\infty}} = 1$ and $\overline{X_{\infty}} = 1 - \Lambda$ (equation 44). Because $\overline{Y_{\infty}} = 1$ the material balance reads $\overline{X}(T) = 1 - \Lambda \cdot U(T)$ (equation 32). When $\Lambda > 1$ the solid phase is in excess and $\overline{X_{eq}} = 0$, while the local solid phase concentration changes by time, i.e., $Y_{R=1}$ varies (Figure 17). Thus the constant solid phase concentration condition at the external surface area of the solid becomes invalid, i.e., the boundary condition at the solid external

surface is time-dependent. At global equilibrium $\overline{X_\infty} = 0$ and $\overline{Y_\infty} = {}^{1}/_{\Lambda}$. Finally, the material balance reads $\overline{X}(T) = 1 - U(T)$.

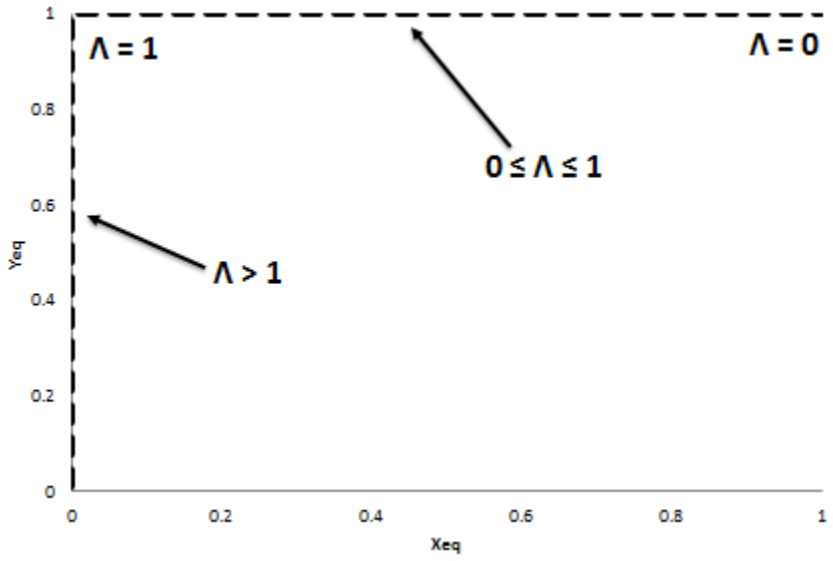

Figure 16. Rectangular isotherm representation.

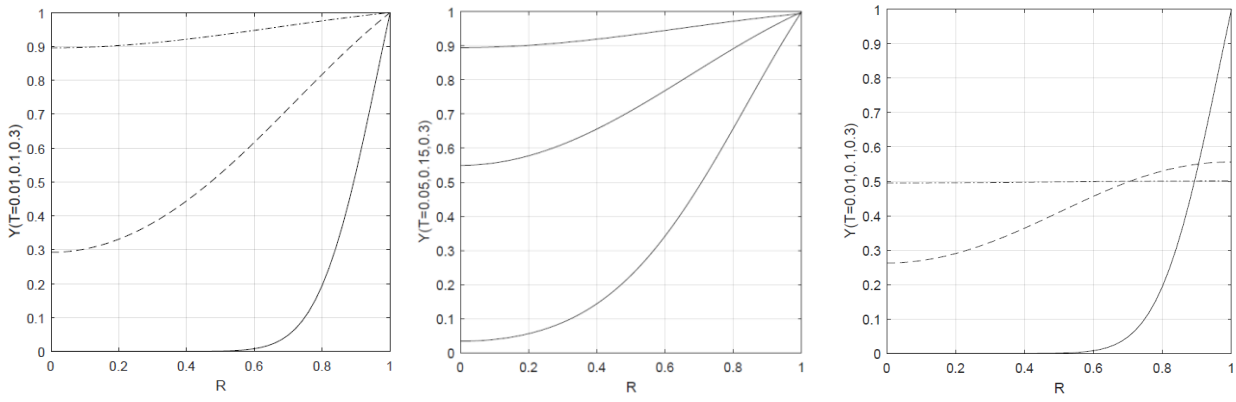

Figure 17. Solid phase concentration profiles for Bi = 100 and irreversible isotherm (p = 1, K_1 = 5000, K_2 = 1) for Λ = 0.5 (left), Λ = 1 (middle) and Λ = 2 (right)

Thus, Boyd's equation (69) holds in the case of surface diffusion control, finite solution volume, $\Lambda \leq 1$ and rectangular isotherm. The concentration in the fluid phase is given by using the material balance [1]:

$$\bar{X}(T) = 1 - \Lambda \cdot \left[1 - \frac{6}{\pi^2} \cdot \sum_{n=1}^{\infty} \frac{1}{n^2} \cdot \exp(-n^2 \cdot \pi^2 \cdot T)\right] \tag{70}$$

In Figure 18 the numerical solution for the irreversible isotherm is compared with the favorable isotherms and Boyd's equation. As expected, for $\Lambda = 0.9$ the solution for irreversible equilibrium coincides with Boyd's equation due to the boundary condition at R = 1, but for $\Lambda = 2$ Boyd's equation diverges as the boundary condition becomes time-dependent.

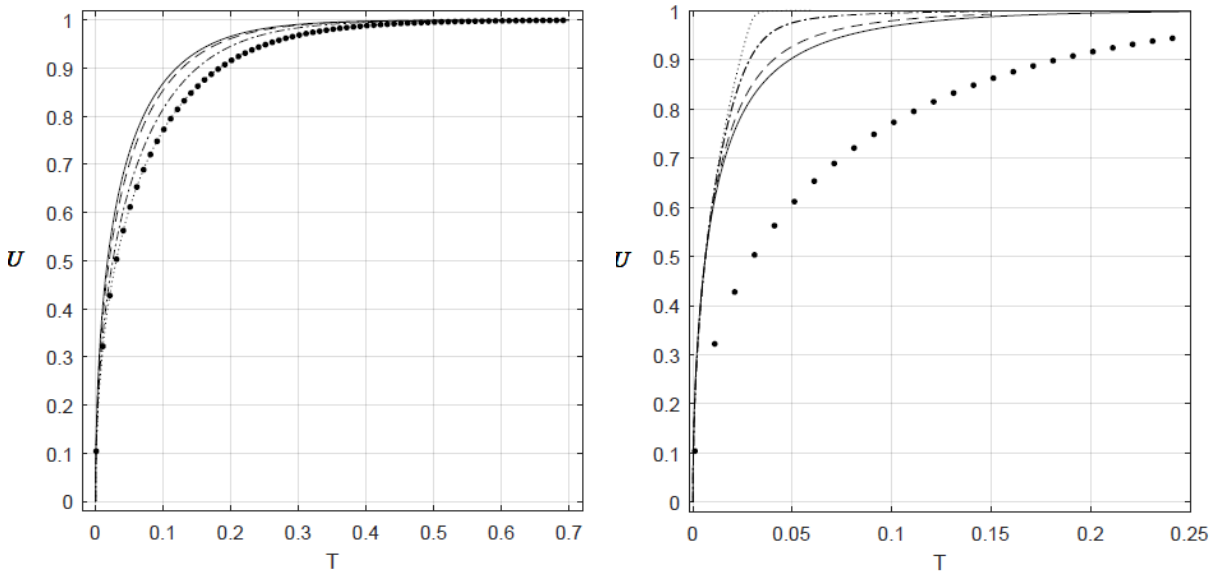

Figure 18. Boyd's equation (points) and numerical solution for Bi = 100 and $\Lambda = 0.9$ (left) and $\Lambda = 2$ (right) for different favorable DSM isotherms: $p = 1/K_1 = 5/K_2 = 1$ (solid), $p = 1/K_1 = 10/K_2 = 1$ (dashed), $p = 1/K_1 = 50/K_2 = 1$ (dashed-dot) and $p = 1/K_1 = 5000/K_2 = 1$ (irreversible - dotted).

As far as ion exchange is concerned, rigorous ion exchange kinetic models superimpose the electric transference on ordinary diffusion driven by the concentration gradient, as described by

the Nernst-Planck theory [61]. An infinite solution volume version of the Nernst-Plank model was presented by Helfferich [6]:

$$U(T) = \{1 - \exp[\pi^2 \cdot f_1(a_i) \cdot T_A + f_2(a_i) \cdot T_A^2 + f_3(a_i) \cdot T_A^3]\}^{0.5} \quad (71)$$

The dimensionless time (T_A) is:

$$T_A = \frac{D_A \cdot t}{r_p^2} \quad (72)$$

where D_A is the surface diffusion coefficient of the incoming ion (A). The parameter a_i is the ratio of the surface diffusion coefficients of the incoming ion (A) to the ion initially in the solid phase (B). The functions f_1, f_2 and f_3 take several forms depending on the valences of the ions. For example, for univalent-bivalent exchange and $1 < a_i < 20$:

$$f_1(a) = -\frac{1}{0.64 + 0.36 \cdot a^{0.668}} \quad (73)$$

$$f_2(a) = -\frac{1}{0.96 - 2 \cdot a^{0.4685}} \quad (74)$$

$$f_3(a) = -\frac{1}{0.27 + 0.09 \cdot a^{1.14}} \quad (75)$$

For univalent-bivalent exchange the isotopic exchange model (Boyd's equation) can be used instead of the more complex ion exchange model (Nernst-Plank) under certain conditions [29]. However, away from the infinite solution volume condition, ion exchange kinetics depend on selectivity, and Crank's equation is not valid unless the isotherm is linear (isotopic exchange). Nernst-Plank model has been occasionally used without always examining the infinite solution volume condition. Some examples of the applications of this model include the isotopic exchange of molybdate ions on calcium molybdate [62], the adsorption of dyes onto zeolites [63], and the removal of U(VI) by hydrogels [64]. A review of several ion exchange kinetics models is presented in Petruzzelli et al. [61].

Finally, Perry and Green [54] give the following equation for fluid film diffusion control, infinite solution volume condition, and Langmuir isotherm:

$$\left(1-\frac{1}{K_1}\right)\cdot U(T)-\left(\frac{1}{K_1}\right)\cdot \ln[1-U(T)]=3\cdot Bi\cdot T \tag{76}$$

Langmuir isotherm is equivalent to the DSM for $0 \leq (1/K_1) \leq 1$, $K_2 = 1$ and $p = 1$. The solution for linear isotherm ($K_1 = 1$) is given by Boyd et al. (1947) [57]. Note that when the fluid film diffusion step is involved, the isotherm is needed as the boundary condition at R = 1 becomes concentration-dependent. The comparison of numerical and analytical solutions for fluid film diffusion control are provided in Figure 19. The agreement between the models is perfect. Again, the effect of the isotherm is profound and for rectangular isotherm the U(T)-T curve becomes linear.

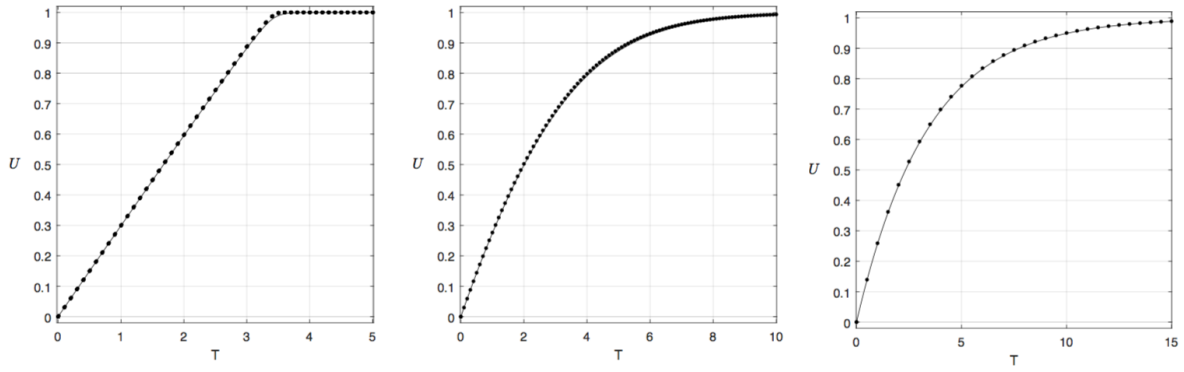

Figure 19. Comparison of the numerical solution (solid line) and Perry & Green's equation (points) for Bi = 0.1 and $\Lambda = 0.01$. Left: $(1/K_1) = 0$ (irreversible equilibrium), Middle: $(1/K_1) = 0.5$ (favorable equilibrium) and Right: $(1/K_1) = 1$ (linear isotherm).

2.7 Approximate solutions to the HSDM

Paterson (1947) worked out an approximation to his finite solution volume equation for linear isotherm or isotopic exchange [6]:

$$U(T) = \frac{\Lambda+1}{\Lambda} \cdot \left\{1 - \frac{1}{a-b} \cdot \left[a \cdot exp(a^2 \cdot T) \cdot \left(1 + erf(a \cdot T^{0.5})\right) - b \cdot exp(b^2 \cdot T) \cdot \left(1 + erf(b \cdot T^{0.5})\right)\right]\right\} \quad (77)$$

where α and b are the roots of the equation:

$$x^2 + 3 \cdot \Lambda \cdot x - 3 \cdot \Lambda = 0 \quad (78)$$

Crank's equation (60) and Paterson's approximation give practically the same results for the entire range of U(T) with an error of 0.001-0.005 for 0.5≤Λ≤2. Paterson's approximation has been used in isotopic exchange studies, as for example the exchange of sodium and cesium ions on hydrous zirconia [65], sodium and cesium ions on titanium(IV) antimonite [66], and molybdate ions on calcium molybdate [62]. Furthermore, it has been used for systems that follow non-linear isotherms, such as the removal of organic cations by clinoptilolite [67], the ion exchange of calcium on zeolite A [68], the ion exchange of several metals on clinoptilolite [69], the adsorption of a herbicide on bituminous shale [70], the adsorption of basic dye onto zeolitic materials synthesized from fly ash [63], the removal of U(VI) by hydrogels [64], the ion exchange of copper on weak acid resins [71], and the adsorption of Cr(VI) on sawdust [72]. A discussion on this issue is done later in this section.

Concerning ion exchange, Inglezakis and Grigoropoulou [29] showed that Paterson's approximation can provide an acceptable estimate of the surface diffusion coefficients in ion exchange systems under certain conditions. It is important to underline that in the definition of Λ, Helfferich is using the term "*total concentration of counter ions*" for $\overline{C_o}$ and $\overline{q_o}$ [6]. In ion exchange, both concentrations, if expressed as normality, are constant during the exchange as the phenomenon is stoichiometric. Paterson [73], originally working on a heat transfer problem, also uses the respective constant properties of the two phases, i.e., heat capacities. However, this has

caused misinterpretations in literature. The reason is that the total concentration of counter ions in the solid phase is the real exchange capacity (REC) that may or may not be available for exchange under specific experimental conditions [44]. However, in the adsorption models the equilibrium solid phase concentration ($\overline{q_o}$) corresponding to a fluid phase equilibrium concentration equal to ($\overline{C_o}$) is used which is equivalent to the the maximum exchange level (MEL). The later expresses the concentration of the solid phase counter ions actually exchangeable under the specific initial liquid phase concentration ($\overline{C_o}$).

Under the infinite solution volume condition, Vermeulen's approximation can be used [6]:

$$U(T) = [1 - \exp(-\pi^2 \cdot T)]^{0.5} \tag{79}$$

Vermeulen's and Boyd's equation (69) give practically the same results the whole range of U(T) with an error of 0.0045. Vermeulen's approximation has been frequently used without always observing the infinite solution volume condition. For example, Viegas et al. [74] discuss the applicability of Vermeulen's approximation for the adsorption on carbons and compares it to the HSDM model, without mentioning the infinite solution volume condition. Trgo et al. [75] apply the model to zinc and lead ion exchange on a zeolite, Naiya et al. [76] to the adsorption of metal ions onto clarified sludge, and Sarkar and Bandyopadhyay [77] to the adsorption of dyes on rice husk ash, but the infinite solution volume condition was not verified, and most probably were not met.

Inglezakis and Grigoropoulou [29] showed that Vermeulen's approximation can be used for ion exchange systems under infinite solution volume conditions and also for isotopic exchange and finite solution volume with acceptable errors for $\Lambda < 0.1$ and $\alpha < 20$, provided that is applied in the range of U(T) of 0.3-0.8. The lower limit depends on Λ and the higher limit attains a higher value depending on the lower U(T) limit. However, as is common in the literature, the error was

calculated as the vertical distance between the U(T) predictions of the models, i.e., the error for the same T, which amplifies the error when T is small as the U(T)-T curves have large slope. The upper limit depends on a_i and is relevant to the assumption of the constant surface diffusion coefficient. The higher the value of a_i the lower the upper limit should be (see also section 2.5.3). Inglezakis and Grigoropoulou [29]argued that Paterson's approximation can be used for any U(T) value up to 0.8, depending on a_i. Although an upper limit in the vicinity of 0.7 is used in several publications, the conclusion derived by Inglezakis and Grigoropoulou [29] was based on the comparison of the isotopic and ion exchange infinite solution volume models, not on the comparison of finite solution volume solutions. The experiments performed in the same publication, as in several others mentioned above, showed that Paterson's approximation can give satisfactory estimation of surface diffusion coefficients for ion exchange systems away from the isotopic exchange/linear isotherm condition, for an upper limit of U(T) around 0.9. The question then is why the approximations based on linear isotherms are working in non-linear isotherm systems?

In order to facilitate the discussion, the effect of the isotherm on the numerical solution for Bi = 100 (surface diffusion control) and Bi = 0.1 (fluid film diffusion control) are presented in Figures 20 and 21. As is evident, for low U(T) values the distance between the curves is not large. Focusing on the surface diffusion control case, which is the most common, it is clear that for U(T)<0.7 the distance between the numerical solutions for linear (representing Crank's equation) and non-linear isotherms is negligible (Table 3). Also, for $\Lambda = 0.4$ Boyd's equation perfectly fits the numerical solution for the strongly favorable isotherm for the whole range of U(T). This is expected as discussed in section 2.6.2 in the analysis of the surface diffusion control, finite solution volume, $\Lambda \leq 1$ and irreversible isotherm.

Table 3. Error (distance between the curves) for Bi = 100.

Curves	Λ = 0.4		Λ = 2	
	0<U(T)<0.7	**0.7<U(T)<1**	**0<U(T)<0.7**	**0.7<U(T)<1**
Linear-Boyd	0.0039	0.0083	0.0113	0.0296
Strongly favorable-Boyd	0.00031	0.0006	0.0142	0.0413
Strongly favorable-linear	0.005	0.0115	0.0005	0.012

Although the results depend on the type of isotherm and value of (Λ), it can be concluded that the analytical and approximate solutions can be used up to a certain limit of U(T). This upper limit of U(T) depends not only on the linearity of the isotherm but also on the concentration dependence of the surface diffusion coefficient (see section 2.5.3).

These results justify the use of analytical and approximate equations, but the pitfalls must be highlighted and a discussion on the fitting of a non-linear model is necessary. The constant diffusivity TP-HSDM used to derive the above results is a parametric non-linear model, whose solutions are a function of the independent variable T and a set of parameters (Λ, Bi, p, K_1, K_2), which are typically known except the one used as a fitting parameter. The convergence of two solutions of such a model does not necessarily mean that the fitting parameter is the same; the convergence alone is merely indicting that the model is insensitive to this parameter for a range of the independent variable. The difference is that the results presented above are generated for the same fitting parameter. In an adsorption experiment the initial fluid concentration ($\overline{C_o}$), fluid volume (V_L), solid's properties (r_p and ρ_p), solid mass (M), and the isotherm ($\overline{q_o}$, p, K_1, K_2) are known while, in the typical case, the fluid phase mass transfer coefficient (k_f) is calculated by use of correlations. Thus, the only unknown parameter is the solid phase diffusion coefficient

(D_s) which is the fitting parameter of the model. The above analysis shows that different numerical solutions converge up to a value of U(T) for the same Λ and Bi, which in practice are calculated by use of the experimental values and the D_s, which is the same for all solutions. In this case the solutions are interchangeable, meaning that if they are applied to an experimental kinetic curve up to a certain U(T), they will give similar fit quality and D_s. Clearly, the application of a simplified model, which is not in agreement with the system's physical reality (the isotherm in this case), is justified only when the objective is the estimation of the D_s, and conclusions should not be extended to the mechanism of the process.

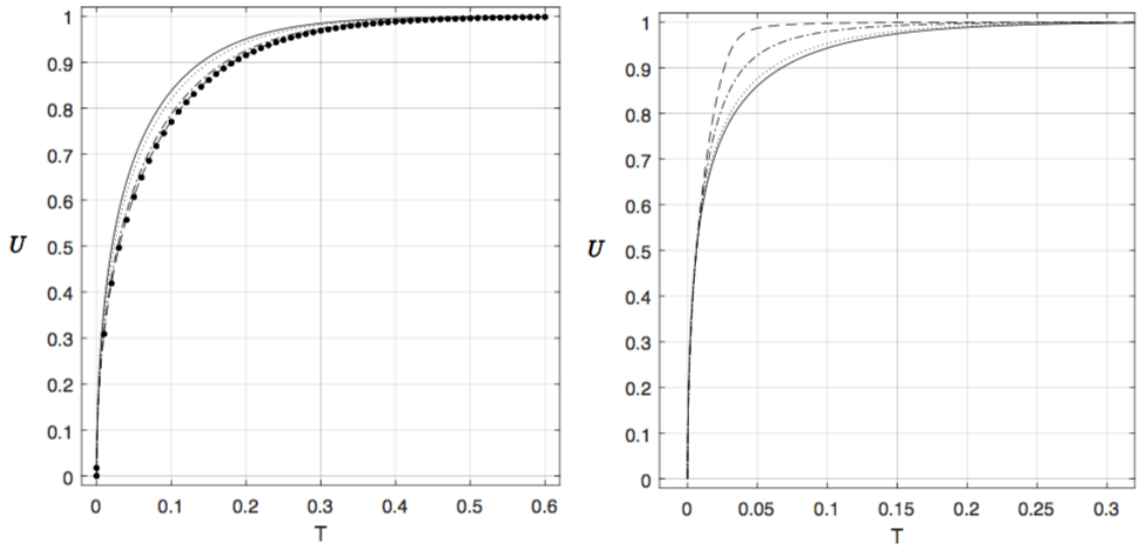

Figure 20. Effect of the isotherm on the numerical solution for Bi = 100 (surface diffusion control). Left: Λ = 0.4 (points for Boyd's equation) and Right: Λ = 2 for different DSM isotherms: $p = 1/K_1 = 100/K_2 = 1$ (dashed line-strongly favorable), $p = 1/K_1 = 10/K_2 = 1$ (dashed-dot line), $p = 1/K_1 = 2/K_2 = 1$ (dotted line) and $p = 1/K_1 = 1/K_2 = 1$ (solid line - linear isotherm).

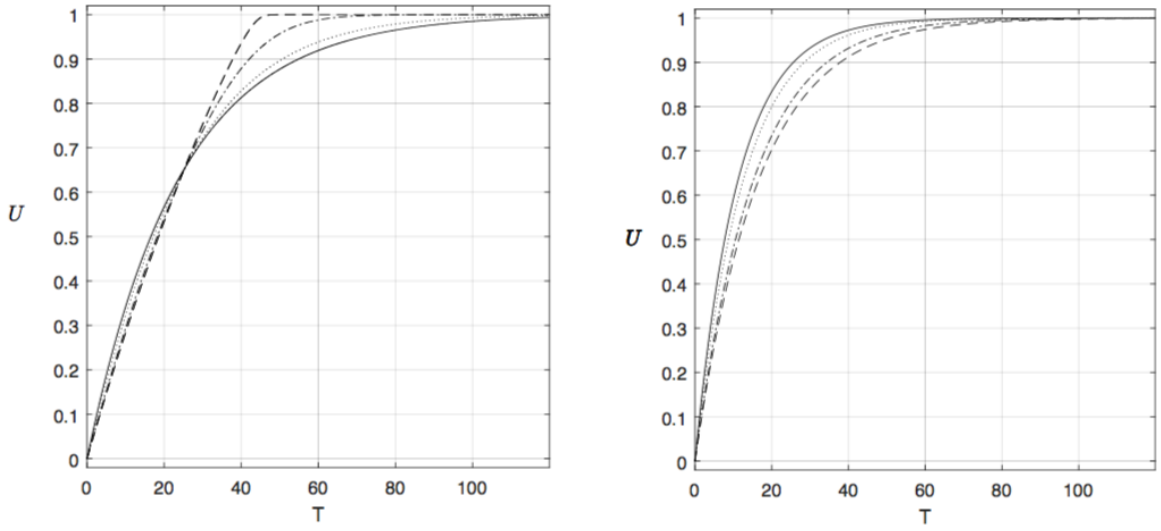

Figure 21. Effect of the isotherm on the numerical solution for Bi = 0.1 (fluid film diffusion control). Left: Λ = 0.4 and Right: Λ = 2 for different DSM isotherms: p = $1/K_1$ = $100/K_2$ = 1 (dashed line-strongly favorable), p = $1/K_1$ = $10/K_2$ = 1 (dashed-dot line - favorable), r = $1/K_1$ = $2/K_2$ = 1 (dotted line – slightly favorable) and p = $1/K_1$ = $1/K_2$ = 1 (solid line - linear isotherm).

While Paterson's and Vermeulen's equations are approximations of the HSDM model this of Glueckauf (1955) is based on the linear driving force (LDF) approximation. This implies the substitution of Fick's diffusion equation (6) with the following one [78]:

$$\frac{d\overline{q_t}}{dt} = k \cdot \left(q_{t,r=r_p} - \overline{q_t} \right) \tag{80}$$

where $q_{t,r=r_p}$ is the solid phase concentration that would be in equilibrium with the instantaneous (at time t) fluid phase concentration, i.e., an imaginary solid phase equilibrium concentration (see Figure 2). The constant (k_G) has a physical meaning and is related to the surface diffusion coefficient as follows:

$$k_G = \frac{g \cdot D_S}{r_p^2} \tag{81}$$

where (g) is a constant that Glueckauf set equal to 15 [79]. For a linear equilibrium an analytical solution is possible:

$$U(T) = 1 - \exp\left[-\frac{g \cdot T \cdot (1+A)}{A}\right] \tag{82}$$

For infinite solution volume $A \rightarrow \infty$ the above equation becomes:

$$U(T) = 1 - \exp(-g \cdot T) \tag{83}$$

Glueckauf's model is valid for $T > 0.1$ [80]. This model is not as common as other adsorption diffusion-based models in literature, but it has been applied in a number of systems, such as for the ion exchange of nickel and zinc on Amberlite IR-120 resin [81]. Glueckauf's equation with g=15 and Vermeulen's equation were successfully applied by El-sharkawy et al. [60] on the kinetics of a mixture of pentafluoroethane, 1,1,1,2-tetrafluoroethane, and difluoromethane onto granular activated carbon. Jribi et al. [82] studied the adsorption of CO_2 on activated carbon and found that the LDF equation with a constant mass transfer coefficient cannot fit the experimental data. Hence, they proposed a solid phase concentration-dependent mass transfer coefficient. A comparison of equation (83) with Vermeulen's equation shows that the two equations converge for g = 20.06, but the errors are significant (Figure 22). Sircar and Hufton [78] evaluated the LDF model and concluded that although the shape is similar to the HSDM analytical solutions for the finite solution volume, there is a lack of quantitative fit with the divergence being a function of g.

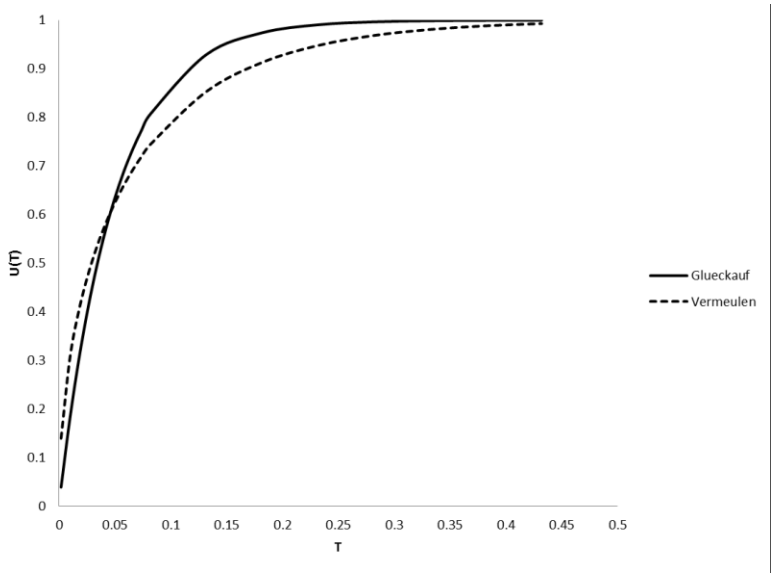

Figure 22. Comparison of Glueckauf and Vermeulen equations for g = 20.06.

3. Reaction-diffusion based models

An important theoretical model is the shrinking core model (SCM), which has been successfully used to describe the rate of a variety of processes, including sorption [53]. This model was originally proposed by Yagi and Kunii [83] and later modified by Wen [84] and Levenspiel [85] for non-catalytic solid-fluid chemical reactions. According to the model, the reaction occurs first at the outer skin of the particle (core) and moves into the solid, leaving behind completely converted material and inert solid (shell) (Figure 23). The solid is initially non-porous, and as the reaction advances the shell becomes porous while the core remains non-porous [84]. The model assumes an irreversible first order reaction (rectangular isotherm), takes into account both fluid and solid phase (pore fluid) diffusion steps, and assumes steady state diffusion in the solid phase.

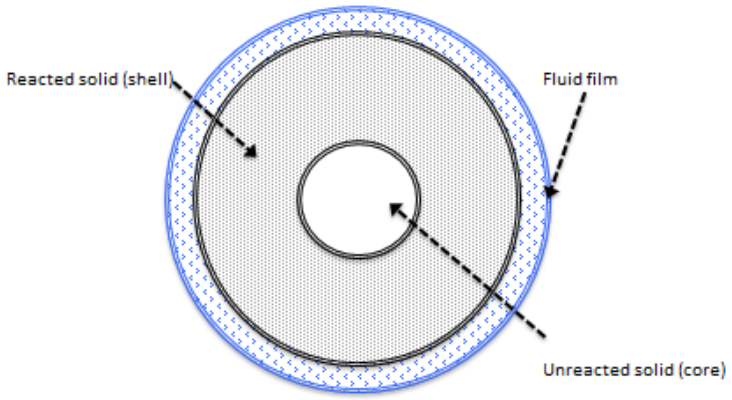

Figure 23. SCM graphical representation.

The reaction considered in the classic form of the model is [85]:

$$A(fluid) + bB(so1id) \rightarrow products$$

The fractional conversion can be defined as:

$$X_r = 1 - \left(\frac{r_c}{r_p}\right)^3 = \frac{\overline{q_t}}{\overline{q_m}} \tag{84}$$

where r_c is the core radius and $\overline{q_m}$ is the initial concentration of reactant B. In adsorption terminology, $\overline{q_m}$ represents the maximum possible loading of the solid phase with the incoming solute (binding sites), is constant and for an irreversible reaction (rectangular isotherm), and is analogous to saturation capacity Q_m. If equilibrium is attained, then, $\overline{q_m}$ is the final equilibrium solid phase concentration $\overline{q_\infty}$, and X_r becomes equal to the fractional attainment of equilibrium U(t) (equation 49).

Originally, the model was derived for constant fluid phase concentration, i.e., infinite solution volume but it has been adapted for the finite solution condition [51,53,86,87]. Under the assumptions stated above, the solution of the model for fluid film diffusion control is:

$$X_r = \frac{3 \cdot b \cdot k_f}{\rho_p \cdot \overline{q_m} \cdot r_p} \cdot \int_0^t \overline{C_t} dt \tag{85}$$

For pore diffusion control:

$$1 - 3 \cdot (1 - X_r)^{2/3} + 2 \cdot (1 - X_r) = \frac{6 \cdot b \cdot D_p}{\rho_p \cdot \overline{q_m} \cdot r_p^2} \cdot \int_0^t \overline{C_t} dt \quad (86)$$

For chemical reaction control:

$$1 - (1 - X_r)^{1/3} = \frac{b \cdot k_r}{\rho_p \cdot \overline{q_m} \cdot r_p} \cdot \int_0^t \overline{C_t} dt \quad (87)$$

where b is the stoichiometric coefficient of the reaction and k_r the chemical reaction rate constant. The equations presented were developed for a simple reaction, but when the reaction is fast they can be used for any reaction type as the mechanism becomes irrelevant. In this case, the SCM solutions for fluid film and pore diffusion control become essentially diffusion-based models [86]. Hence, for chemisorption and ion exchange, accompanied by a fast irreversible chemical reactions (rectangular isotherm), the SCM model is suitable and independent of the reaction mechanism. The shrinking core concept has been used with purely diffusion-based models and irreversible equilibrium for the derivation of analytical solutions. For instance, the infinite solution volume version of pore diffusion control (equation 86) can represent the PDM under an infinite solution volume condition and a rectangular isotherm [1,36]. Other diffusion-based models can be also used when the reaction rate is fast, however, the physical significance is compromised.

The existence of sharp advancing fronts in ion exchange systems is observed in several systems, and this led to the routine application of the SCM. However, as Helfferich [88] underlines, there must be some physical cause for the shell-core boundary to remain sharp, and this cannot be other than a fast chemical reaction that immobilizes the entering species on the core's periphery preventing them from penetrating further. An example of such reaction is the complexation of metal ions by fixed chelating groups in resins. The assumption of a non-porous core further

ensures the absence of diffusion towards the center of the solid. If the solid is porous, the solute can diffuse freely into it and the SCM becomes invalid [53,84]. In this case the solute interacts with the solid's surface homogeneously throughout the solid producing a gradual variation of concentration in the particle. Another weakness of the SCM is the assumption of steady state diffusion in the pores' fluid phase, which implies that equation (17) becomes [84]:

$$0 = D_p \cdot \left(\frac{\partial^2 C_p}{\partial r^2} + \frac{2}{r} \cdot \frac{\partial C_p}{\partial r} \right) \tag{88}$$

where D_p is the pore diffusion coefficient. Note that SCM is based on the PDM discussed in section 2.2. The steady state diffusion condition in the pores means that the shrinkage of the unreacted core is slower than the transfer rate of the solute towards the unreacted core. Under this condition the unreacted core can be considered as stationary [85]. Wen [84] states that the pseudo-steady state approximation is valid for most of the solid-gas reaction systems but not for solid-liquid systems unless the liquid reactant concentration is very low.

There are some studies where the SCM is used, as for instance in Rao and Gupta [86] for the ion exchange of heavy metals on chelating resins, Dicinoski et al. [89] for the kinetics of gold, silver and nickel cyanide complexes onto anion exchange resins, Inglezakis et al. [87] for the ion exchange of Pb^{2+} on a chelating resin, Barzamini et al. [90] for the adsorption of mercaptans on zeolites, and Sancho et al. [91] for the removal of ammonia from aqueous solutions on membranes and a zeolite. McKay [92] developed an analytical solution for combined fluid and solid phase diffusion resistances and applied it on the adsorption of a basic dye on silica. The SCM's weaknesses however are obvious; irreversible equilibrium and pseudo-state solid diffusion assumptions are not met in many systems. For instance, Chen et al. [51] applied SCM on the removal of Cu^{2+} on calcium alginate gel and found that the derived diffusion coefficients were unrealistic as a result of invalid assumptions made by the SCM. Consequently, the SCM

has been modified to accommodate different types of isotherms, but the solutions are only numerical. Jena et al. [34] presented a modified SCM based on the PDM under the pseudo-state assumption, which is applicable for any isotherm. This model was applied on the adsorption of astrazone blue dye on silica, para-nitrophenol on granular activated carbon, toluene on activated carbon [34], the adsorption of metals onto sludge [76], arsenic adsorption on natural laterite [93], and the adsorption of dyes on rice husk ash [77]. Maria and Mansur [94] studied the removal of manganese on bone char and applied a modified form of the SCM based on the PDM, with Langmuir isotherm and the pseudo-state state assumption in the solid phase. The results using the SCM were erroneous as they showed that the solid/liquid ratio affects the pore phase diffusion coefficient. Pritzker [53] presented a modified SCM based on HSDM (see section 2.1) to account for an incompletely reacted shell. The model is valid for any isotherm under the pseudo-state state assumption in the solid phase. Pritzker [53] applied the modified SCM on the removal of Cu^{2+} ions onto calcium alginate gel. In Figure 24, the solid phase concentration profiles of the SCM and modified SCM for pore diffusion control are shown for comparison. Wen [84] presents SCM-HSDM combined models, applicable mostly for solid phase non-catalytic reactions.

The major difference between SCM, HSDM and PDM is that in SCM the adsorbate is rapidly and totally adsorbed at the shell-core interface, i.e., the shell is inert to the diffusing species and the core is free of solute, while in HSDM and PDM diffusion happens in all points of the solid. Also, in PDM the adsorbent concentration gradient is due to a combination of diffusion and equilibrium in all points, in HSDM a combination of equilibrium at the fluid-solid interface and diffusion, in modified SCM a combination of diffusion and equilibrium in the shell, and in SCM

a consequence of diffusion alone. The result is that models display continuous but dissimilar solute concentration gradients as shown in Figure 24.

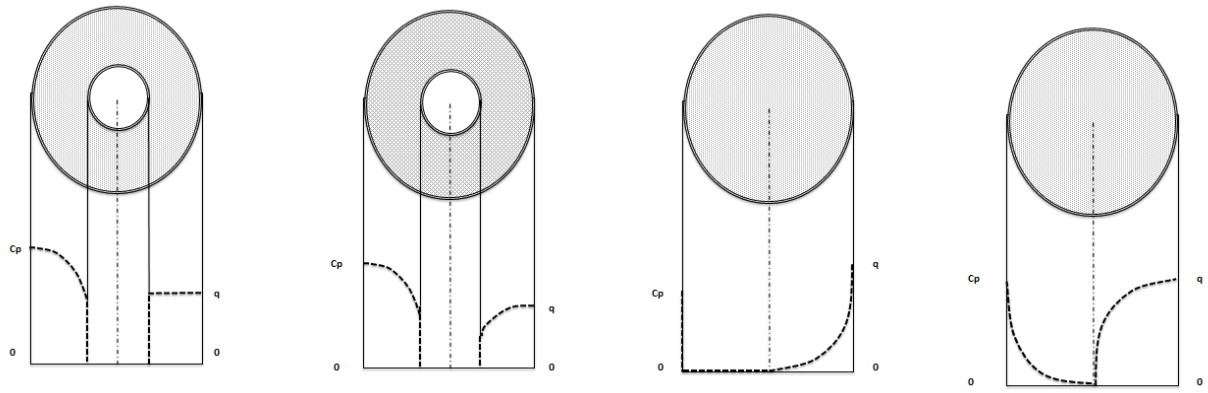

Figure 24. Intraparticle concentration profiles. From left to right: SCM, modified SCM, HSDM and PDM.

In HSDM, a concentration profile is developing in the solid phase reaching the center of the solid and gradually becomes horizontal as it moves closer to equilibrium over time (Figure 9). For small T the HSDM gives a profile that progressively moves towards the center, resembling the modified SCM, but the curvatures of the two profiles are different (Figure 24). Furthermore, as Chen et al. [51] and Priztker [53] showed, the HSDM profile penetrates the solid phase and reaches its center much faster than the SCM profile. This is a result of the assumptions behind the models; the entire solid phase is available for diffusion in HSDM but only the shell in SCM. The differences between the SCM and HSDM hold for the rectangular isotherm as well.

Another reaction-diffusion based model is the Langmuir kinetics model (LKM), which is theoretical and the basis of Langmuir isotherm [5]:

$$\frac{d\bar{q_t}}{dt} = k_L \cdot \left[\bar{C_t} \cdot (Q_m - \bar{q_t}) - \frac{1}{b_L} \cdot \bar{q_t}\right] \tag{89}$$

where k_L is the Langmuir rate coefficient and b_L a constant. The model is valid for systems that follow the Langmuir isotherm, which is derived from equation (89) at equilibrium for $d\overline{q_t}/dt = 0$. The solution to the LKM is:

$$\overline{X} = \frac{\overline{C_t}}{\overline{C_o}} = 1 - \frac{\gamma \cdot (\alpha - \beta)}{\overline{C_o}} \cdot \left\{ \frac{1 - \exp(-2 \cdot \gamma \cdot \beta \cdot k_L \cdot t)}{1 - \left[\frac{\alpha - \beta}{\alpha + \beta}\right] \cdot \exp(-2 \cdot \gamma \cdot \beta \cdot k_L \cdot t)} \right\} \tag{90}$$

where, γ is the solid mass M to liquid volume V_L ratio and:

$$\alpha = \frac{1}{2} \cdot \left(\frac{\overline{C_o}}{\gamma} + Q_m + \frac{1}{b_L \cdot \gamma} \right) \tag{91}$$

$$\beta = \left(\alpha^2 - \frac{\overline{C_o} \cdot Q_m}{\gamma} \right)^{0.5} \tag{92}$$

The Langmuir rate coefficient k_L is a lumped parameter which accounts for both the intrinsic adsorption kinetics and mass transfer steps and Chu [5] showed that the solid phase diffusion coefficient can be estimated by using the following equation:

$$\frac{1}{k_L} \simeq \frac{r_p^2 \cdot \rho_p \cdot Q_m \cdot \left(\frac{1}{1 + b_L \cdot \overline{C_o}} + 1 \right)}{30} \cdot \left[\frac{5}{k_f \cdot r_p} + \frac{1}{\left(\frac{D_s \cdot \rho_p \cdot q_o}{\overline{C_o}} \right)} \right] \tag{93}$$

The equilibrium constant La in equation (28) is related to the LKM constant b_L as follows:

$$La = \frac{1}{1 + b_L \cdot \overline{C_o}} \tag{94}$$

LKM was successfully applied for the adsorption of pyridine on activated carbon and 5-hydroxymethylfurfural and acrylonitrile on a polymeric resin [5]. Also, Al-Jabari [95] used LKM in combination to fluid film diffusion resistance for fitting experimental results for the adsorption of Cr^{3+} on marlstone and stone cutting particles.

4. Reaction kinetics-based models

Most of the reaction kinetics-based models consider the adsorption kinetics on the surface of the solid phase assuming that mass transfer is fast enough to be neglected. Strictly speaking, these models are applicable in chemisorption on solids that are either non-porous or porous exhibiting high diffusion coefficients. Excellent reviews on the use of these models for the adsorption of organic and inorganic pollutants from water/wastewater are these of Febrianto et al. [12], Gupta and Bhattacharyya [4], Malamis and Katsou [96], and Tan and Hameed [27].

Probably the most popular model of this type is the pseudo-first-order (PFO) rate equation of Lagergren which originally appear in literature in 1898 [25]:

$$\frac{d\overline{q_t}}{dt} = k \cdot (\overline{q_\infty} - \overline{q_t}) \tag{95}$$

where k is the reaction rate constant. After integration:

$$\ln\left(\frac{\overline{q_\infty}}{\overline{q_\infty} - \overline{q_t}}\right) = k \cdot t \tag{96}$$

The PFO model has been extensively used in adsorption studies, including the adsorption of metal ions on a large number of inorganic materials and biosorbents [12,96]. The first order kinetic processes signify reversible interactions with an equilibrium being established between fluid and solid phases [4]. The PFO model has the same form as the linear driving force (LDF) diffusion-based model of Glueckauf (equation 80); however, the models are equivalent only when the isotherm is linear and under the infinite solution volume condition [97]. This is happening because the driving force in the solid film, used in Glueckauf's model, is the difference between the surface concentration $q_{t,r=rp}$ and the average solid loading at time t (Figure 2), while in the PSO model it is the difference between the true equilibrium $\overline{q_{eq}}$ and the average loading of the solid at time t [35]. Despite its simplicity and relativelly sucessful implementation in many systems, Lagergren's model is criticized in a number of papers as theoretically inconsistent.

Tran et al. [10] discussed a number of reaction kinetics-based models, including the pseudo-second-order rate equation (PSO), which was first presented by Blanchard et al. in 1984 [98] :

$$\frac{d\overline{q_t}}{dt} = k \cdot (\overline{q_\infty} - \overline{q_t})^2 \quad (97)$$

After integration:

$$\frac{1}{\overline{q_\infty} - \overline{q_t}} = \frac{1}{\overline{q_\infty}} + k \cdot t \quad (98)$$

The PSO model assumes that the rate-limiting step is most likely to involve chemical interactions leading to the binding of the ions to the surface by strong covalent bonding [4]. PSO has been extensively used on several studies, such as the removal of metals by use of inorganic materials and biosorbents [12,96].

Elovich's equation was first proposed by and Roginsky and Zeldovich in 1934 [99] for the adsorption of carbon monoxide onto manganese dioxide and it has been used for chemisorption:

$$\frac{d\overline{q_t}}{dt} = a_k \cdot e^{-b \cdot \overline{q_t}} \quad (99)$$

where a_k is the initial adsorption rate and b is the desorption constant. The integrated form of this equation is [100]:

$$\overline{q_t} = \frac{1}{b} \cdot \ln\left(t + \frac{1}{a_k \cdot b}\right) - \frac{1}{b} \cdot \ln\left(\frac{1}{a_k \cdot b}\right) \quad (100)$$

According to several researchers, the Elovich equation is suitable for highly heterogeneous sorbents and is based on the assumption that the sorption sites increase exponentially with sorption, which implies a multilayer sorption, and each layer exhibits a different activation energy for chemisorption [101]. In comparison to PFO and PSO models, Elovich's equation is only occasionally used, for instance, for the adsorption of Cd(II) on natural clinoptilolite and hexadecyltrimethylammonium-clinoptilolite [4]. Wu et al. [100] provided a comparison between Elovich, Lagergren and Weber-Moris equations.

The models presented above are empirical in nature and, as Tan and Hameed [27] noted, most publications focus on the solid material employed, and the kinetic models serve merely to complement the adsorbent evaluation and, inevitably, the origins, strengths, limitations, and interpretation of the underlying phenomena are not addressed. Rudzinski and Plazinski [102] showed that they are simplified forms of a more general theoretical equation when the adsorption kinetics is governed by the rate of surface reactions. However, the analysis is based on completely different physical assumptions and can not be interpreted as general one. Azizian [103] theoretically derived the PFO and SFO rates as special cases of the Langmuir adsorption rates. Plazinski [11] and Tan and Hameed [27] rightfully argue that these models do not represent any specific mechanism, that they lack physical significance, and that they are simply highly flexible mathematical formulas able to fit well kinetic curves. The shape of the experimental kinetics curves can be easily represented with several equations having two fitting constants, and this is why the kinetic models can be sucessful in many cases [22]. It is also true that researchers often ignore the assumptions of reaction kinetics-based models and evaluate their applicability solely on the quality of the fit on the experimental data [104]. This has been nicely illustrated by Ocampo-Perez et al. [20], who studied phenol adsorption on organobentonite; the results showed that the reaction kinetic-based models fitted the experimental data reasonably well, but the derived kinetic parameters varied with experimental conditions without any physical significance or plausible explanation. Thus the answer to the question Simonin [17] poses on the PFO and PSO models "*which of the two rate laws better describes an adsorption process controlled by diffusion?*" is plainly "*none*".

The analytical and approximate models discussed in this paper are summarized in Table 4.

Table 4. Summary of analytical and approximate models

Model (equation)	Isotherm	Controlling step	Chemical reaction	Solution volume
Chemical kinetics-based				
PFO (96)	None	Chemical reaction	Yes	Finite
PSO (98)	None	Chemical reaction	Yes	Finite
Elovich (100)	None	Chemical reaction	Yes	Finite
LKM (90)	Langmuir	Adsorption reaction	No	Finite
SCM (85-87) SCM (86)	Rectangular Rectangular	Any single Pore diffusion	Yes No	Finite Infinite
Mass transfer diffusion-based				
Crank (60) Paterson (77)	Linear	Surface/Pore diffusion	No	Finite
Boyd (69) Vermeulen (79)	Any Linear Rectangular	Surface/Pore diffusion	No	Infinite Finite ($A \leq 1$)
Glueckauf (82)	Linear	Surface diffusion	No	Finite
Weber and Moris (1)	Linear	Surface diffusion	No	Infinite
Nernst-Plank (71)	Any	Surface diffusion	No	Infinite
Perry and Green (76)	Langmuir Linear Rectangular	Fluid film diffusion	No	Infinite
Helfferich (67)	Linear	Fluid film diffusion	No	Finite

5. Conclusions

A new versatile variable diffusivity two-phase homogeneous diffusion model incorporating a flexible non-linear isotherm is presented and used for the evaluation of the analytical and approximate models. The numerical model is equipped with the Chen-Yang variable diffusivity correlation, which can deal with both increasing and decreasing surface diffusion coefficients

with increasing solid loading. Due to the non-linearity of the boundary condition at the surface of the solid phase, analytical solutions are possible only for constant intraparticle diffusion coefficient and linear or rectangular isotherms unless the volume of the solution is infinite. The weaknesses of the analytical diffusion-based models include the assumption of a constant solid phase diffusion coefficient and the limitations on the isotherm shape. Nevertheless, the comparison of the analytical models to the numerical solution demonstrated that the deviation can be small away from equilibrium, i.e. for U(T) lower than 0.5-0.7, depending on the system. This upper limit of U(T) depends on the linearity of the isotherm, the controlling diffusion step (Biot number) and the blockage of the solid's pores (hindered diffusion). Clearly, the application of a simplified model, which is not in accordance with the system's physical reality, i.e. the constant diffusion coefficient or the isotherm is justified only when the objective is the estimation of the solid phase diffusion coefficient and conclusions should not be extended to the mechanism of the process. Despite their weaknesses, reaction kinetics-based models are easy to use and can provide some insights into the adsorption mechanism, if applied carefully in well-designed experiments. Also, under the range of experimental conditions they are applied, they can be used for process design. The LKM and the SCM are superior to the empirical kinetics-based models but are not as widely applied as the later.

It is imperative to underline that the adsorption mechanisms cannot be directly assigned by simply fitting kinetic models; a good knowledge of the surfaces and interactions involved supported by analytical techniques, such as XPS, FTIR and SEM, are necessary. As Helfferich [88] puts it "*Even a faulty model can usually be made to fit a limited number of experimental results by adjustment of its parameters. However, if it seriously violates physical reality, it is apt to produce erroneous predictions and conclusions.*".

Acknowledgements

This work has been financially supported by the ORAU project "*Hyperstiochiometry Activity in Metal Nanoparticle Interaction (HYPERActiv)*", SOE2015009, Nazarbayev University and the HORIZON 2020 project "*Nanoporous and Nanostructured Materials for Medical Applications (NanoMed)*", H2020-MSCA-RISE-2016, 734641, European Commission. The author Marios M. Fyrillas was partially supported by CRoNoS – IC408 COST Action.

6. References

[1] M. Suzuki, Adsorption engineering, 1990. doi:10.1016/0923-1137(91)90043-N.
[2] A. Zagorodni, Ion Exchange Materials: Properties and Applications, 1st editio, Elsevier, 2007.
[3] M. Schwaab, E. Steffani, E. Barbosa-Coutinho, J.B. Severo Júnior, Critical analysis of adsorption/diffusion modelling as a function of time square root, Chem. Eng. Sci. 173 (2017) 179–186. doi:10.1016/j.ces.2017.07.037.
[4] S. Sen Gupta, K.G. Bhattacharyya, Kinetics of adsorption of metal ions on inorganic materials: A review, Adv. Colloid Interface Sci. 162 (2011) 39–58. doi:10.1016/j.cis.2010.12.004.
[5] K.H. Chu, Extracting surface diffusion coefficients from batch adsorption measurement data: application of the classic Langmuir kinetics model, Environ. Technol. (United Kingdom). 0 (2017) 1–10. doi:10.1080/09593330.2017.1397767.
[6] F.G. Helfferich, Ion Exchange, Dover science books, 1962.
[7] Q. Zhang, J. Crittenden, K. Hristovski, D. Hand, P. Westerhoff, User-oriented batch reactor solutions to the homogeneous surface diffusion model for different activated carbon dosages, Water Res. 43 (2009) 1859–1866. doi:10.1016/j.watres.2009.01.028.
[8] P.K. Pandey, S.K. Sharma, S.S. Sambi, Removal of lead(II) from waste water on zeolite-NaX, J. Environ. Chem. Eng. 3 (2015) 2604–2610. doi:10.1016/j.jece.2015.09.008.
[9] G.F. Malash, M.I. El-Khaiary, Piecewise linear regression: A statistical method for the analysis of experimental adsorption data by the intraparticle-diffusion models, Chem. Eng. J. 163 (2010) 256–263. doi:10.1016/j.cej.2010.07.059.
[10] H.N. Tran, S.J. You, A. Hosseini-Bandegharaei, H.P. Chao, Mistakes and inconsistencies regarding adsorption of contaminants from aqueous solutions: A critical review, Water Res. 120 (2017) 88–116. doi:10.1016/j.watres.2017.04.014.
[11] W. Plazinski, Binding of heavy metals by algal biosorbents. Theoretical models of kinetics, equilibria and thermodynamics, Adv. Colloid Interface Sci. 197–198 (2013) 58–67. doi:10.1016/j.cis.2013.04.002.
[12] J. Febrianto, A.N. Kosasih, J. Sunarso, Y.H. Ju, N. Indraswati, S. Ismadji, Equilibrium

and kinetic studies in adsorption of heavy metals using biosorbent: A summary of recent studies, J. Hazard. Mater. 162 (2009) 616–645. doi:10.1016/j.jhazmat.2008.06.042.
[13] L. Largitte, R. Pasquier, A review of the kinetics adsorption models and their application to the adsorption of lead by an activated carbon, Chem. Eng. Res. Des. 109 (2016) 495–504. doi:10.1016/j.cherd.2016.02.006.
[14] P.R. Souza, G.L. Dotto, N.P.G. Salau, Detailed numerical solution of pore volume and surface diffusion model in adsorption systems, Chem. Eng. Res. Des. 122 (2017) 298–307. doi:10.1016/j.cherd.2017.04.021.
[15] Y.S. Ho, G. McKay, A Comparison of chemisorption kinetic models applied to pollutant removal on various sorbents, Process Saf. Environ. Prot. 76 (1998) 332–340. doi:10.1205/095758298529696.
[16] J.D. Le Roux, A.W. Brysont, B.O. Youngt, A comparison of several kinetic models for the adsorption of gold cyanide onto activated carbon, J. South African Inst. Min. Metall. 91 (1991) 95–103. doi:10.1007/BF03216558.
[17] J.P. Simonin, On the comparison of pseudo-first order and pseudo-second order rate laws in the modeling of adsorption kinetics, Chem. Eng. J. 300 (2016) 254–263. doi:10.1016/j.cej.2016.04.079.
[18] G.J. Millar, G.L. Miller, S.J. Couperthwaite, S. Dalzell, D. Macfarlane, Determination of an engineering model for exchange kinetics of strong acid cation resin for the ion exchange of sodium chloride & sodium bicarbonate solutions, J. Water Process Eng. 17 (2017) 197–206. doi:10.1016/j.jwpe.2017.04.011.
[19] V.J. Inglezakis, The physical significance of simplified models in engineering, Model. Optim. Mach. Build. F. 2 (2007) 338–341.
[20] R. Ocampo-Perez, R. Leyva-Ramos, J. Mendoza-Barron, R.M. Guerrero-Coronado, Adsorption rate of phenol from aqueous solution onto organobentonite: Surface diffusion and kinetic models, J. Colloid Interface Sci. 364 (2011) 195–204. doi:10.1016/j.jcis.2011.08.032.
[21] G.L. Dotto, C. Buriol, L.A.A. Pinto, Diffusional mass transfer model for the adsorption of food dyes on chitosan films, Chem. Eng. Res. Des. 92 (2014) 2324–2332. doi:10.1016/j.cherd.2014.03.013.
[22] R. Leyva-Ramos, R. Ocampo-Pérez, J.V. Flores-Cano, E. Padilla-Ortega, Comparison between diffusional and first-order kinetic model, and modeling the adsorption kinetics of pyridine onto granular activated carbon, Desalin. Water Treat. 55 (2015) 637–646. doi:10.1080/19443994.2014.920278.
[23] V.J. Inglezakis, M.M. Fyrillas, Adsorption fixed beds modeling revisited: Generalized solutions for S-shaped isotherms, Chem. Eng. Commun. (2017). doi:10.1080/00986445.2017.1364240.
[24] G. Marbán, L.A. Ramírez-Montoya, H. García, J.Á. Menéndez, A. Arenillas, M.A. Montes-Morán, Load-dependent surface diffusion model for analyzing the kinetics of protein adsorption onto mesoporous materials, J. Colloid Interface Sci. 511 (2018) 27–38. doi:10.1016/j.jcis.2017.09.091.
[25] Y.S. Ho, Review of second-order models for adsorption systems, J. Hazard. Mater. 136 (2006) 681–689. doi:10.1016/j.jhazmat.2005.12.043.
[26] H. Qiu, L. Lv, B. Pan, Q. Zhang, W. Zhang, Q. Zhang, Critical review in adsorption kinetic models, J. Zhejiang Univ. A. 10 (2009) 716–724. doi:10.1631/jzus.A0820524.
[27] K.L. Tan, B.H. Hameed, Insight into the adsorption kinetics models for the removal of

contaminants from aqueous solutions, J. Taiwan Inst. Chem. Eng. 74 (2017) 25–48. doi:10.1016/j.jtice.2017.01.024.
[28] T.W. Weber, Batch adsorption for pore diffusion with film resistance and an irreversible isotherm, Can. J. Chem. Eng. 56 (1978) 187–196. doi:10.1002/cjce.5450560206.
[29] V.J. Inglezakis, H.P. Grigoropoulou, Applicability of simplified models for the estimation of ion exchange diffusion coefficients in zeolites, J. Colloid Interface Sci. 234 (2001). doi:10.1006/jcis.2000.7304.
[30] V. Meshko, L. Markovska, M. Mincheva, A.E. Rodrigues, Adsorption of basic dyes on granular activated carbon and natural zeolite, Water Res. 35 (2001) 3357–3366. http://www.ncbi.nlm.nih.gov/pubmed/11547856.
[31] Z. Xu, J. Cai, B. Pan, Mathematically modeling fixed-bed adsorption in aqueous systems, J. Zhejiang Univ. Sci. A. 14 (2013) 155–176. doi:10.1631/jzus.A1300029.
[32] V. Russo, R. Tesser, M. Trifuoggi, M. Giugni, M. Di Serio, A dynamic intraparticle model for fluid-solid adsorption kinetics, Comput. Chem. Eng. 74 (2015) 66–74. doi:10.1016/j.compchemeng.2015.01.001.
[33] D.D. Do, Adsorption Analysis: Equilibria and Kinetics, 1998. doi:10.1142/p111.
[34] P.R. Jena, J.K. Basu, S. De, A generalized shrinking core model for multicomponent batch adsorption processes, Chem. Eng. J. 102 (2004) 267–275. doi:10.1016/j.cej.2003.12.006.
[35] E. Worch, Adsorption technology in water treatment: Fundamentals, processes, and modeling, 2012. doi:10.1515/9783110240238.
[36] D.M. Ruthven, Principles of Adsorption and Adsorption Processes, John Wiley & Sons, 1984.
[37] D. Do, R. Rice, On the relative importance of pore and surface diffusion in non equilibrium adsorption rate process, Chem. Eng. Sci. 42 (1987) 2269–2284.
[38] J.G. Choi, D.D. Do, H.D. Do, Surface diffusion of adsorbed molecules in porous media: Monolayer, multilayer, and capillary condensation regimes, Ind. Eng. Chem. Res. 40 (2001) 4005–4031. doi:10.1021/ie010195z.
[39] Y.D. Chen, R.T. Yang, Concentration-Dependence of Surface-Diffusion and Zeolitic Diffusion, AIChE J. 37 (1991) 1579–1582.
[40] D.C.K. Ko, C.W. Cheung, J.F. Porter, A branched pore kinetic model applied to the sorption of metal ions on bone char, J. Chem. Technol. Biotechnol. 80 (2005) 861–871. doi:10.1002/jctb.1196.
[41] X. Yang, S.R. Otto, B. Al-Duri, Concentration-dependent surface diffusivity model (CDSDM): Numerical development and application, Chem. Eng. J. 94 (2003) 199–209. doi:10.1016/S1385-8947(03)00051-2.
[42] R.M. Barrer, J. Klinowski, Ion-exchange selectivity and electrolyte concentration, J. Chem. Soc. Faraday Trans. 1 Phys. Chem. Condens. Phases. 70 (1974) 2080–2091. doi:10.1039/F19747002080.
[43] R.P. Dyer, A., Enamy, H., Townsend, The Plotting and Interpretation of Ion-Exchange Isotherms in Zeolite Systems, Sep. Sci. Technol. 16 (1981) 173–183. doi:10.1080/01496398108058111.
[44] V.J. Inglezakis, The concept of “capacity” in zeolite ion-exchange systems, J. Colloid Interface Sci. 281 (2005). doi:10.1016/j.jcis.2004.08.082.
[45] V.J. Inglezakis, M.M. Fyrillas, M.A. Stylianou, Two-phase homogeneous diffusion model for the fixed bed sorption of heavy metals on natural zeolites, Microporous Mesoporous Mater. 266 (2018). doi:10.1016/j.micromeso.2018.02.045.

[46] O. Bricio, J. Coca, H. Sastre, Effect of the Heterogeneity of Macroporous Styrene-Dvb Resins on Ion-Exchange Equilibria, Solvent Extr. Ion Exch. 15 (1997) 647–664. doi:10.1080/07366299708934499.
[47] F. Pepe, D. Caputo, C. Colella, The Double Selectivity Model for the Description of Ion-Exchange Equilibria in Zeolites, Ind. Eng. Chem. Res. 42 (2003) 1093–1097. doi:10.1021/ie020512h.
[48] C.F. Gerald, P.O. Wheatley, Applied Numerical Analysis, 1994.
[49] W.E. Deming, Statistical Adjustment of Data, Wiley, New York, 1943.
[50] J. Crank, The mathematics of diffusion, 2nd ed., Clarendon Press, Oxford, 1975.
[51] D. Chen, Z. Lewandoswki, F. Roe, P. Surapaneni, Diffusivity of Cu2+ in calcium alginate gel beads., Biotechnol. Bioeng. 41 (1993) 755–760. doi:10.1002/bit.260430212.
[52] M.M. Araújo, J.A. Teixeira, Trivalent chromium sorption on alginate beads, Int. Biodeterior. Biodegrad. 40 (1997) 63–74. doi:10.1016/S0964-8305(97)00064-4.
[53] M. Pritzker, Modified shrinking core model for uptake of water soluble species onto sorbent particles, Adv. Environ. Res. 8 (2004) 439–453.
[54] P. S, R.H. Perry, D.W. Green, J.O. Maloney, Chemical Engineers ' Handbook Seventh, 1997. doi:10.1021/ed027p533.1.
[55] A.E. Kurtoğlu, G. Atun, Determination of kinetics and equilibrium of Pb/Na exchange on clinoptilolite, Sep. Purif. Technol. 50 (2006) 62–70. doi:10.1016/j.seppur.2005.11.008.
[56] A. Dyer, K.J. White, Cation diffusion in the natural zeolite clinoptilolite, Thermochim. Acta. 341 (1999) 1–7. doi:10.1016/S0040-6031(99)00280-4.
[57] G.E. Boyd, J. Schubert, A.W. Adamson, The Exchange Adsorption of Ions from Aqueous Solutions by Organic Zeolites. Ion-exchange Equilibria, J. Am. Chem. Soc. 69 (1947) 2818–2829. doi:10.1021/ja01203a064.
[58] M. Šljivić Ivanovic, I. Smičiklas, S. Pejanović, Analysis and comparison of mass transfer phenomena related to Cu2+sorption by hydroxyapatite and zeolite, Chem. Eng. J. 223 (2013) 833–843. doi:10.1016/j.cej.2013.03.034.
[59] T. Motsi, N.A. Rowson, M.J.H. Simmons, Kinetic studies of the removal of heavy metals from acid mine drainage by natural zeolite, Int. J. Miner. Process. 101 (2011) 42–49. doi:10.1016/j.minpro.2011.07.004.
[60] M.M. El-Sharkawy, A.A. Askalany, K. Harby, M.S. Ahmed, Adsorption isotherms and kinetics of a mixture of Pentafluoroethane, 1,1,1,2-Tetrafluoroethane and Difluoromethane (HFC-407C) onto granular activated carbon, Appl. Therm. Eng. 93 (2016) 988–994. doi:10.1016/j.applthermaleng.2015.10.077.
[61] D. Petruzzelli, F. Helfferich, L. Liberti, G. Millar, R. Passino, Kinetics of ion exchange with intraparticle rate control: Models accounting for interactions in teh solid phase, React. Polym. 7 (1987) 1–13.
[62] G. Atun, B. Bilgin, A. Kilislioglu, Kinetics of isotopic exchange between strontium polymolybdate and strontium ions in aqueous solution, Appl. Radiat. Isot. 56 (2002) 797–803. doi:10.1016/S0969-8043(02)00052-0.
[63] G. Atun, G. Hisarli, A.E. Kurtoğlu, N. Ayar, A comparison of basic dye adsorption onto zeolitic materials synthesized from fly ash, J. Hazard. Mater. 187 (2011) 562–573. doi:10.1016/j.jhazmat.2011.01.075.
[64] S. Ortaboy, E.T. Acar, G. Atun, S. Emik, T.B. Iyim, G. Güçlü, S. Özgümüş, Performance of acrylic monomer based terpolymer/montmorillonite nanocomposite hydrogels for U(VI) removal from aqueous solutions, Chem. Eng. Res. Des. 91 (2013) 670–680.

doi:10.1016/j.cherd.2012.12.007.
[65] I.M. El-Naggar, M.I. El-Dessouky, H.F. Aly, Self-diffusion and ionic transport of sodium and cesium ions in particles of hydrous zirconia, Solid State Ionics. 57 (1992) 339–343. doi:10.1016/0167-2738(92)90167-N.
[66] S.A. Shady, B. El-Gammal, Diffusion pathways of sodium and cesium ions in the particles of titanium(IV) antimonate, Colloids Surfaces A Physicochem. Eng. Asp. 268 (2005) 7–11. doi:10.1016/j.colsurfa.2005.01.036.
[67] R.M. Barrer, R. Papadopoulos, L.V.C. Rees, Exchange of sodium in clinoptilolite by organic cations, J. Inorg. Nucl. Chem. 29 (1967) 2047–2063. doi:10.1016/0022-1902(67)80466-4.
[68] D. Drummond, A. De Jonge, L.V.C. Rees, Ion-exchange kinetics in zeolite A, J. Phys. Chem. 87 (1983) 1967–1971. doi:10.1021/j100234a027.
[69] V.J. Inglezakis, M.M. Loizidou, H.P. Grigoropoulou, Ion exchange studies on natural and modified zeolites and the concept of exchange site accessibility, J. Colloid Interface Sci. 275 (2004). doi:10.1016/j.jcis.2004.02.070.
[70] N. Ayar, B. Bilgin, G. Atun, Kinetics and equilibrium studies of the herbicide 2,4-dichlorophenoxyacetic acid adsorption on bituminous shale, Chem. Eng. J. 138 (2008) 239–248. doi:10.1016/j.cej.2007.06.032.
[71] C. Modrogan, A.R. Miron, O.D. Orbulet, C. Costache, G. Apostol, Ion Exchange Processes on Weak Acid Resins for Wastewater Containing Cooper Ions Treatment, Environ. Eng. Manag. J. 14 (2015) 449–454.
[72] L. Mukosha, M. Onyango, A. Ochieng, J. Siame, Effective Microporosity for Enhanced Adsorption Capacity of Cr (VI) from Dilute Aqueous Solution: Isotherm and Kinetics, Chem. Sci. Int. J. 19 (2017) 1–12. doi:10.9734/CSJI/2017/34082.
[73] S. Paterson, The heating or cooling of a solid sphere in a well-stirred fluid, Proc. Phys. Soc. 59 (1947) 50–58. doi:10.1088/0959-5309/59/1/310.
[74] R.M.C. Viegas, M. Campinas, H. Costa, M.J. Rosa, How do the HSDM and Boyd's model compare for estimating intraparticle diffusion coefficients in adsorption processes, Adsorption. 20 (2014) 737–746. doi:10.1007/s10450-014-9617-9.
[75] M. Trgo, J. Perić, N.V. Medvidović, A comparative study of ion exchange kinetics in zinc/lead-modified zeolite-clinoptilolite systems, J. Hazard. Mater. 136 (2006) 938–945. doi:10.1016/j.jhazmat.2006.01.032.
[76] T.K. Naiya, A.K. Bhattacharjee, D. Sarkar, S.K. Das, Applicability of shrinking core model on the adsorption of heavy metals by clarified sludge from aqueous solution, Adsorption. 15 (2009) 354–364. doi:10.1007/s10450-009-9186-5.
[77] D. Sarkar, A. Bandyopadhyay, Shrinking Core Model in characterizing aqueous phase dye adsorption, Chem. Eng. Res. Des. 89 (2011) 69–77. doi:10.1016/j.cherd.2010.04.010.
[78] S. Sircar, J.R. Hufton, Why does the linear driving force model for adsorption kinetics work?, Adsorption. 6 (2000) 137–147. doi:10.1023/A:1008965317983.
[79] S. Sircar, J.R. Hufton, Intraparticle adsorbate concentration profile for linear driving force model, AIChE J. 46 (2000) 659–660. doi:10.1002/aic.690460325.
[80] H.K. Hsuen, An improved linear driving force approximation for intraparticle adsorption, Chem. Eng. Sci. 55 (2000) 3475–3480. doi:10.1016/S0009-2509(99)00600-4.
[81] P.E. Franco, M.T. Veit, C.E. Borba, G. da C. Gonçalves, M.R. Fagundes-Klen, R. Bergamasco, E.A. da Silva, P.Y.R. Suzaki, Nickel(II) and zinc(II) removal using Amberlite IR-120 resin: Ion exchange equilibrium and kinetics, Chem. Eng. J. 221 (2013)

426–435. doi:10.1016/j.cej.2013.02.006.
[82] S. Jribi, T. Miyazaki, B.B. Saha, A. Pal, M.M. Younes, S. Koyama, A. Maalej, Equilibrium and kinetics of CO2adsorption onto activated carbon, Int. J. Heat Mass Transf. 108 (2017) 1941–1946. doi:10.1016/j.ijheatmasstransfer.2016.12.114.
[83] S. Yagi, D. Kunii, Theory on roasting of sulfide ore with uniform particle diameter in fluidized beditle, Kogyou-Kagaku-Zassi. 56 (1953) 131.
[84] C.Y. Wen, Noncatalytic heterogeneous solid-fluid reaction models, Ind. Eng. Chem. 60 (1968) 34–54. doi:10.1021/ie50705a007.
[85] O. Levenspiel, Chemical Reaction Engineering, John Wiley and Sons, New York, 1972.
[86] M.G. Rao, A.K. Gupta, Ion exchange processes accompanied by ionic reactions, Chem. Eng. J. 24 (1982) 181–190. doi:10.1016/0300-9467(82)80033-6.
[87] V.J. Inglezakis, M.D. Loizidou, H.. Grigoropoulou, Pb2+ removal from liquid phase using chelating resin lewatit TP 207: The effect of operating variables and application of shrinking core model, in: 8th Int. Conf. Environ. Sci. Technol., 2003: pp. 341–348.
[88] F.G. Helfferich, Models and physical reality in ion-exchange kinetics, React. Polym. 13 (1990) 191–194. doi:10.1016/0923-1137(90)90053-7.
[89] G.W. Dicinoski, L.R. Gahan, P.J. Lawson, J.A. Rideout, Application of the shrinking core model to the kinetics of extraction of gold (I), silver (I) and nickel (II) cyanide complexes by novel anion exchange resins, Hydrometallurgy. 56 (2000) 323–336.
[90] R. Barzamini, C. Falamaki, R. Mahmoudi, Adsorption of ethyl, iso-propyl, n-butyl and iso-butyl mercaptans on AgX zeolite: Equilibrium and kinetic study, Fuel. 130 (2014) 46–53. doi:10.1016/j.fuel.2014.04.013.
[91] I. Sancho, E. Licon, C. Valderrama, N. de Arespacochaga, S. López-Palau, J.L. Cortina, Recovery of ammonia from domestic wastewater effluents as liquid fertilizers by integration of natural zeolites and hollow fibre membrane contactors, Sci. Total Environ. 584–585 (2017) 244–251. doi:10.1016/j.scitotenv.2017.01.123.
[92] G. McKay, Analytical solution using a pore diffusion model for a pseudoirreversible isotherm for the adsorption of basic dye on silica, AIChE J. 30 (1984) 692–697. doi:10.1002/aic.690300434.
[93] A. Maiti, H. Sharma, J.K. Basu, S. De, Modeling of arsenic adsorption kinetics of synthetic and contaminated groundwater on natural laterite, J. Hazard. Mater. 172 (2009) 928–934. doi:10.1016/j.jhazmat.2009.07.140.
[94] M.E. Maria, M.B. Mansur, Mathematical modeling of batch adsorption of manganese onto bone char, Brazilian J. Chem. Eng. 33 (2016) 373–382. doi:10.1590/0104-6632.20160332s20140077.
[95] M. Al-Jabari, Kinetic models for adsorption on mineral particles comparison between Langmuir kinetics and mass transfer, Environ. Technol. Innov. 6 (2016) 27–37. doi:10.1016/j.eti.2016.04.005.
[96] S. Malamis, E. Katsou, A review on zinc and nickel adsorption on natural and modified zeolite, bentonite and vermiculite: Examination of process parameters, kinetics and isotherms, J. Hazard. Mater. 252–253 (2013) 428–461. doi:10.1016/j.jhazmat.2013.03.024.
[97] A.E. Rodrigues, C.M. Silva, What's wrong with Lagergreen pseudo first order model for adsorption kinetics?, Chem. Eng. J. 306 (2016) 1138–1142. doi:10.1016/j.cej.2016.08.055.
[98] G. Blanchard, M. Maunaye, G. Martin, Removal of heavy metals from waters by means of

natural zeolites, Water Res. 18 (1984) 1501–1507. doi:10.1016/0043-1354(84)90124-6.
[99] S. Roginsky, Y.B. Zeldovich, The catalytic oxidation of carbon monoxide on manganese dioxide, Acta Physico-Chemica Sin. 1 (1934) 554.
[100] F.C. Wu, R.L. Tseng, R.S. Juang, Characteristics of Elovich equation used for the analysis of adsorption kinetics in dye-chitosan systems, Chem. Eng. J. 150 (2009) 366–373. doi:10.1016/j.cej.2009.01.014.
[101] G. Alberti, V. Amendola, M. Pesavento, R. Biesuz, Beyond the synthesis of novel solid phases: Review on modelling of sorption phenomena, Coord. Chem. Rev. 256 (2012) 28–45. doi:10.1016/j.ccr.2011.08.022.
[102] W. Rudzinski, W. Plazinski, Kinetics of solute adsorption at solid/solution interfaces: A theoretical development of the empirical pseudo-first and pseudo-second order kinetic rate equations, based on applying the statistical rate theory of interfacial transport, J. Phys. Chem. B. 110 (2006) 16514–16525. doi:10.1021/jp061779n.
[103] S. Azizian, Kinetic models of sorption: A theoretical analysis, J. Colloid Interface Sci. 276 (2004) 47–52. doi:10.1016/j.jcis.2004.03.048.
[104] Y. Xiao, J. Azaiez, J.M. Hill, Erroneous Application of Pseudo-Second-Order Adsorption Kinetics Model: Ignored Assumptions and Spurious Correlations, Ind. Eng. Chem. Res. 57 (2018) 2705–2709. doi:10.1021/acs.iecr.7b04724.